Stony Brook University

A New Method for Design of Geometrically Shaped Structures for Prescribed Electromagnetic Field Distribution

A Dissertation Presented

by

Carlos M. Pereira

to

The Graduate School

in Partial Fulfillment of the Requirements

for the Degree of

Doctor of Philosophy

in

Electrical Engineering

Stony Brook University

December 2015

Stony Brook University

The Graduate School

Carlos M. Pereira

We, the dissertation committee for the above candidate for the Doctor of Philosophy degree, hereby recommend acceptance of this dissertation.

Harbans Singh Dhadwal – Dissertation Advisor
Associate Professor, Department of Electrical and Computer Engineering

K. Wendy Tang – Chairperson of Defense
Associate Professor, Associate Chair, Department of Electrical and Computer Engineering

Ridha Kamoua
Associate Professor, Department of Electrical and Computer Engineering

Jahangir Rastegar
Associate Professor, Department of Mechanical Engineering

This dissertation is accepted by the Graduate School.

Charles Taber
Dean of the Graduate School

Abstract of the Dissertation

A New Method for Design of Geometrically Shaped Structures for Prescribed Electromagnetic Field Distribution

by

Carlos M. Pereira

Doctor of Philosophy

in

Electrical Engineering

Stony Brook University

2015

The contribution of this research work to the body of existing knowledge is a novel design (inverse) method to compute the distribution of fields when electromagnetic waves interact with surfaces. If given a desired distribution of electromagnetic fields (radiation pattern), the design (inverse) method developed will rapidly allow a designer to determine a unique geometric solution which will provide the desired radiation pattern, which is an inverse problem. The method developed can also be used as an analysis tool to analyze radiating or receiving structures with simple and complex

non-linear geometric features. In the extensive literature search provided in this work, others have used analytical methods for computing the distribution of electromagnetic fields when waves propagate and interact with structures. This requires a mathematical framework to be developed using time-harmonic and magnetic fields to solve boundary value problems using closed-form mathematical relationships that only have closed-form solutions for a few simple geometrical shapes. When the geometrical features of a structure contain arbitrary shapes with irregular geometries, finite element methods can also be used as analysis tools to handle any type of geometrical features, however, both of these methods are used to perform analysis of these types of problems and are very time consuming and not suited as design tools to rapidly provide design information on the geometry features that provide a desired electric field distribution.

This revolutionary methodology provides a design tool which currently does not exist in the reviewed published literature. It overcomes deficiencies presented by current analysis tools, such as theoretical, analytical and numerical methods which are capable of analyzing wave propagation and interaction problems, but are not suited to rapidly design geometrical features of radiating or receiving structures.

Contents

List of Figures

Acknowledgements

To start, I would like to thank the faculty of Stony Brook University, in particular the members of my dissertation committee. As a full-time employee at the Armament Research development Engineering Center, Picatinny Arsenal, New Jersey, It had been a few years since I had last taken classes, and the overall graduate experience at SBU reminded me of why I became an engineer in the first place the love of learning and advancing technology and to continue to perfect the art of teaching and mentoring others.

I am especially grateful to my advisor, Dr. Harbans Singh Dhadwal from the Electrical Engineering department and Dr. Jahangir Rastegar from the Mechanical Engineering Department. who guided me through this effort whenever my schedule allowed in between my full time job at Picatinny and at home. A special thanks to Dr. Dake Feng for all of the help and support, I could not have accomplish this goal without their help. I also would like to thank all of the help from other faculty members, Dr. K. Wendy Tang, Dr. Ridha Kamoua and Dr. David Westerfeld who always made themselves available when I needed help.

In closing I would like to thank my wife, Karen and my three sons, Andrew, Kevin and Ryan for sticking with my difficult schedule, impossible at times,

and for staying on message in the accomplishment of my goals and their goals regardless of setbacks, I am immensely proud of how we all moved on through health adversities. Also would like to thanks my parents, in particular my Mom who has always showed perseverance in all of our lives.

Chapter 1

Introduction

1.1 Background

Analytical and numerical methods reviewed in this chapter are extensively used as analysis tools to determine field distribution inside geometrical spaces of arbitrary shapes when subjected to electromagnetic emissions. These methods however cannot be used to design geometrical spaces with the aim of achieving a prescribed field distribution within the designed space. The latter task requires solving an inverse problem which involves unknown geometries and highly nonlinear effects. The new method presented in this thesis is intended for addressing this inverse problem. The method is shown to provide the means of designing geometrical structures that are subjected to certain electromagnetic wave propagation for the purpose of achieving a prescribed field distribution within the space of the designed geometrical structure.

A comprehensive literature review of the fields is presented in this chapter. An overview of the remaining chapters of this thesis is also provided in the

last section of the chapter.

1.2 Medium of Propagation and electromagnetic waves

Electromagnetic waves can travel through vacuum and air or other gasses and are characterized as non-observable waves. Electromagnetic waves can also propagate in material mediums where forms of polarizable dielectrics, magnetizable materials and other conductive mediums with low electron mobility would provide propagation mediums with imperfect conductions. Propagation of electromagnetic plane waves can be described using two time-dependent and interrelated vectors. One vector represents the electric field component and the other represents the magnetic field component of the electromagnetic wave. The two vectors are perpendicular to each other.

1.3 Energy transport by electromagnetic waves

Energy transmitted by an electromagnetic wave can also be transferred to a surface or geometry. When an electromagnetic wave interacts with a surface and these interactions cause charge distribution on the surface with similar time varying characteristics which could achieve resonance when the surface structure is designed as an appropriate antenna. Since these interactions would occur at high frequencies at the wave, the transfer of the energy to the antenna is fast. For example, at a wave frequency of ten Gigahertz, the transfer of energy would occur in less than ten cycles, which would occur in a few

nanoseconds. Thereby the transfer of the information contained in the propagating wave is transferred to the antenna almost instantaneously.

Electromagnetic waves travelling in vacuum or air propagate at a speed which is a function of the space capacitivity or permittivity (ϵ_0) and the free space inductivity or permeability (μ_0). The wave travels at the measured quantity of one over the square root of the capacitivity of free space multiplied by the inductivity of free space, and the result of this calculation is the speed of light c . Vacuum is characterized as the absence of a medium. Electromagnetic waves can propagate and transfer energy in vacuum by producing electric charge vibrations which generate the electric field vector component and by producing charges in motion which generate the magnetic field component. Together the electric field and the magnetic field vectors are interrelated in time and space and can be expressed as a set of four differential equations known as Maxwells equations.

The transfer of energy to interacting surfaces of an object depends on the surface material and the amount of energy carried by the propagated wave. At the point of interaction with the surface of an object, the propagating wave produces a small current, which can serve as a source charge. Then depending on the surface material properties, the energy may be absorbed by the material, and/or scattered and/or propagated back. In the surface interaction process, electric fields are generated by electric charges (current) and magnetic fields are generated by charge motion. As a propagating wave interacts with the surface of an object, the electromagnetic wave produce currents and fields on the object surface depending on the capacitivity (ϵ_0), inductivity (μ_0), and the conductivity (σ) of the surface material. The propagated wave behaves as

an energy source and as it impinges upon the medium particles of the object surface, thereby producing electric charges that oscillate at the wave frequency. The surface medium response to the generated oscillatory current is based on its capacitivity (ϵ_0), inductivity (μ_0) and the conductivity (σ).

Propagation of electromagnetic (EM) waves in free space or any unbounded homogeneous medium has been analyzed using various analytical methods [4]. In many such methods a combination of closed form solutions for some components of the distribution of the scattered electromagnetic fields over a surface is combined with an approximated solution for the remaining terms that are difficult to treat to obtain an approximate overall solution.

Perturbation methods are an example of the methods used in published literature [7]-[16]. Such methods have been applied to both scattering configurations from and through layered structures and the scattering response is obtained as the superposition of single-scattering due to local interactions filtered by the layered structure. Here the filtering action is considered to arise from the interferential effects due to the coherent interactions with the boundaries. The physical meaning of the first-order perturbative approximation in the layered structure context is described [17] and [18]. In these studies, the expansions permit a time domain characterization of the scattering response, since each wave of the series corresponds to a reflection that will be received with a different time delay.

Other methods used to study electromagnetic propagation involves the application of differential form and integral form of Maxwells equations [19], which are used to derive Stratton-Chu and Galerkin formulations. These formulations are suitable for the development of numerical schemes which provide

to obtain distribution of fields. Other theoretical and numerical methods have been based on spatially averaging electric field in the beams with circular aperture [36]. Some closed-form expressions have been derived using these methods.

In another study, electromagnetic wave propagations and interactions with surfaces are formulated using differential forms as a method to represent Maxwells equations and derive appropriate boundary conditions [19]. The formulations presented in this work this work are limited to certain geometric shapes of the interacting surfaces. Approximations to analytical expressions are also made when constructing integral equations for shapes other than square, rectangles or circles. The methods presented in [19] the Stratton Chu integral equations are derived in terms of differential forms. The corresponding Galerkin formulations are also constructed to develop numerical schemes to obtain approximations of field distributions in curvilinear geometries [29]. It is also noted that the lowest order approximations on flat geometries reduce to forms essentially equivalent to the standard Rao-Wilton-Glisson functions. The effect on accuracy has also been investigated.

A theoretical and numerical investigation of the spatially averaged electric field in the beam of a circular aperture is presented in [36]. The investigation leads to closed-form analytical expressions, based on scalar diffraction theory, which describes the spatially averaged electric field in the Fresnel region of a circular aperture excited by a spatially uniform, harmonic plane wave [37]. The expressions ultimately permit a practical way of predicting certain routine electromagnetic measurements. Because the expressions are valid in the Fresnel region, they are also valid in the near field, the far field, and the

Fraunhofer region of a circular aperture [38]. It is also shown that the closed-form expressions contain, as special cases, classic on-axis and far-field results associated with a circular aperture. The analytical expressions are based on a generalization of Fresnel diffraction originally developed by Lommel in the late 1800s [39]. It is also shown that the results obtained from the closed-form expressions compare quite favorably to results obtained from the exact solution computed via the dyadic Greens function approach [36].

Other published work based on vector analysis of the electromagnetic (EM) fields radiated from thin circular geometries such as a circular structure [41] and the study of near field solutions [54] require various assumptions such as a known and constant current distribution on the thin circular antenna structure, places restrictions on the solution and would only apply to circular structures where the radius of the loop is relatively small. It also provide solutions for the near field problem if the induction fields converge rapidly. For circular loops of arbitrary radius a, the authors use a dyadic Greens function to derive the fields [41]. The analysis is claimed to be more general than those published in [42] and [43].

In another study [50], the exact solution of the EM fields in the near and far zones outside the region (where $r > a$) is derived by the use of the spherical Hankel function of the first kind, but also the closed-series form of the EM fields radiated in the near zone is obtained in series of spherical Bessel functions of the first kind. A Fourier cosine series is used to expand an arbitrary current distribution along the loop and the exact representations of the EM radiated fields are obtained in closed form [51]-[52]. Validity of the approximate formulas is discussed. Error analysis based on numerical computations

of the radiated fields is also given to show the accuracy of the limiting cases.

For fields interacting in the near-field, the work reported in [54] assumes a constant current distribution on the circular wire in free space. An exact integration of the vector potential is performed without recourse to approximations. In [55]-[65], with electric and magnetic field components in an infinitesimal model, electromagnetic field components of the constant current circular loop antenna are determined by direct series differentiation. These solutions are valid in the near and also far field, although many terms of the series are needed for convergence.

Fast and robust solutions of the Helmholtz equation (and the Schrodinger equation for two-dimensional systems) is an important class of wave chaos problems [76]. The interaction of a propagated wave with rectangular, elliptical and circular geometries filled with homogeneous medium materials and the resulting distribution of the fields has been calculated in [77] with the boundary conditions due to the cavity surface irregularities. Geometries that are not chaotic or cannot be integrated have been studied in [78]. In particular, wave functions inside the billiard are expressed in terms of a simple expansion of Hankel functions. The study discusses the implementation of the approach and the classical bowtie cavity is considered as a case study to demonstrate the versatility and efficiency of the method. To validate the accuracy, the field distribution and the eigenvalues calculated using this approach are compared to the solution obtained by boundary integral method. Chaotic cavity and related methods have been studied extensively for applications to electromagnetic interference studies and electromagnetic hazards, particularly for devices that are subjected to extreme electromagnetic fields. The main assumption

made when using chaotic methods is that the platform where the cavities are located is much larger in size than the cavities. Because of the high noise floor nature of the extreme electromagnetic dynamic environments, the data collected has been studied using statistical methods [79]-[81].

Electromagnetic fields interacting with apertures of 3-D conducting structures and filled with dielectric materials have been analyzed using equivalence principle methods to formulate the solution in two parts [82]. The first part consisting of the internal region of the 3-D conducting surfaces outlined by the aperture boundaries and the external region of the 3-D conducting surfaces. Integral equations are derived and solved numerically using Method of Moments technique. The Method of Moments numerical technique is applied to both the aperture and the conducting surfaces by dividing the surfaces into triangular patches to best arrive at a solution of the integral equations and the results were validated using various numerical methods.

Using modal expansion techniques for situations where the slot length was much larger than the slot width, field distributions on closed surfaces have been calculated [88], [100], [101]. The method is valid when the slot width is very small compared to the slot length and the approximate field distribution on the slot surface is assumed to be a cosine function. In [102]-[104], the authors used Method of Moments to analyze the fields interacting with long and very narrow slots. A more accurate technique was used in [104] to analyze a uniform microstrip line [104]. In [106] the development of numerical method based on the MoM technique is reported for the analysis of bound and leaky modes on printed structures.

The studies of the interaction of a propagated wave with a perfect elec-

trically conducting circular cylinder is reported in [107]. Using the Uniform theory of diffraction (UTD)-based approach the interaction of incident electromagnetic fields in circular cylinders outside the paraxial has been determined [108]. In regions close to the axis, however, the results become less accurate. A solution to determine the magnetic surface currents both within and outside the paraxial region of a perfectly conducting cylinder has been obtained using an approximation of the Henkel Function by a uniform asymptotic expansion within the spectral range of the relevant Greens function. For cases where the radius of the cylinder is not small, asymptotic solutions that provide a canonical solution of a PEC circular cylinder is a useful technique as supported by [109] which uses the work reported in [115]-[116]. The most accurate method is described in [115] which is based on Debyes approximation. The related work reported in [125] and [126] are complimentary and provides an accurate solution in both the paraxial region and the region outside of it. In [117], it is assumed that the impedance boundary conditions are linear and that the impedance boundary conditions [142]-[148] can be represented by the ratio of the electric field and the magnetic field. Superposition is then used to determine the resulting charge distributions due to electromagnetic wave interactions.

For communicating information and sensor data using radar techniques extensive analysis has been performed using edge slot structures arrays [150]-[157]. Radiation patterns were derived and analyzed using 1D arrays and modeling assuming that the waveguide has infinite length [158]-[159]. These work use modeling methods employing equivalent electric and magnetic currents in the analysis of slot apertures. For 2D modeling of infinitely long waveguide

structures, direct methods were considered in efforts reported in [161]-[162]. However, the solutions presented by these direct methods generate very large equations with numerous unknowns. To perform this analysis more efficiently, a higher-order method of moments (MoM) technique was developed. It was shown that the approach can significantly reduce the number of unknowns. Higher order basis functions have also been used in [163]. The radiation pattern, reflection and transmission coefficients are found to agree with other methods and are found to be accurate. To analyze various types of complex waveguide structures, Galerkin finite element time domain methods have been investigated [164]. It has been shown that using these methods it is possible to analyze complex waveguide structures using tetrahedral patches instead of triangular patches [119]-[181]. In these studies, higher order functions were used to reduce the number of unknowns and thus reduce the number of equations to solve and save computation time. Complicated structures were analyzed by using six-port power dividers, horn monopoles and circular monopoles. As a method to further speed up computation time, local time stepping [164] was used.

Methods for determining how much propagated energy can be absorbed by conductive ferromagnetic wires were investigated in [202]. Both finite and infinite lengths were considered and a detailed analysis of the absorption spectrum of these wire structures were performed. The design and architecture of electromagnetic absorbers were investigated in [203]-[205] and different materials for these absorbers were investigated in [206]-[207] as well as artificial electromagnetic materials [208]-[214]. Methods to formulate the problem in resonant cavities, microstrip lines and coaxial lines are reported in [219]-[221].

The results of the studies were validated using ferromagnetic wires in a rectangular waveguide. The computations used previous work reported in [217], [222], [223], in which scattering problem of infinitesimal ferromagnetic wires and antenna and the electromagnetic response of finite-length wires are studied [211].

In [237], a comprehensive review of various extensions of finite-difference time-domain (FDTD) and finite-element time-domain (FETD) is presented. These studies include electromagnetic wave propagation in complex media including dispersive, anisotropic, inhomogeneous, and also those including the nonlinear properties of the propagation medium. The literature search indicates the difficulties of obtaining analytical solutions [237] and as a result numerical methods are generally needed to discretize Maxwell equations directly onto a 3-D surface in order to resolve boundary conditions at medium interfaces and to define the existence of electric and magnetic fields and how the transfer of energy from an incident traveling wave is either reflected or scattered or transmitted at the medium interface. In [237], examples of complex mediums with inhomogeneous and frequency dispersive properties, such as biological tissues were studied. In addition, electromagnetic wave interaction characterization with earth which involve a random number of medium types such as rocks, dry and wet soil types, snow, water and vegetation present highly complex dielectric materials with complex constitutive parameters are addressed. A comprehensive review of Finite-Element Methods as applied to electromagnetic field problems in complex mediums with special consideration to applications of finite difference time domain methods (FDTD), and finite element time domain (FETD) methods for transient phenomena in com-

plex media is presented in [242]. A comprehensive review of finite methods and spectral methods addressing integral-equations-based boundary element methods in complex media is presented in [238]-[248].

In summary, numerical methods are used to investigate electromagnetic fields and spatial distributions involving structures with arbitrarily shaped geometries and where the conductivity , or the permittivity , or the permeability may vary with sharp transitions [4]-[81]. In such problems, analytical methods are very difficult to impossible to use to obtain closed-form solutions. In short, for simple geometrical shapes such as a circle, cylindrical rectangle or square shapes and simple electromagnetic input waves it may be possible to develop closed-form solutions. However for most cases where the geometry of the structure may be more complex, analytical methods cannot be used to determine charge and fields distributions. In such cases, the only viable option is the use of numerical methods (see for example, [117], [142], [148]).

The contribution of work being reported in this thesis is the development of a new method for the design of structural geometries that when interacting with emitted electromagnetic waves would provide a prescribed field distribution within the structure. The numerical methods that have been developed to date can be used to determine field distribution in a given geometrical structure for a given interacting electromagnetic wave. The contribution of the work being developed is the development of a methods that can solve the inverse of this problem, i.e., determine the structural geometry that can yield a desired field distribution.

Chapter 2 presents the aforementioned developed method in detail together with its theoretical basis and simple example of its implementation. The

design tools described in the Chapter 2 will provide the means to quickly determine an approximate geometry to achieve the desire field distribution. The initially established grid sizes and wave profile approximation and time increments may then be refined to converge the field distribution as closely as possible to the prescribed distribution. In the Chapter 3, several design problem examples are presented and the process of arriving at the desired field distribution is described in detail. The results of the Finite Element modeling and analysis of the designed geometrical structures using ANSYS software validating the designs are also provided. A discussion of the developed method and its potentials, conclusions that can be reached and suggestions for future work are provided in the Chapter 4.

Chapter 2

A New Method for Determining Electromagnetic Field Distribution In Arbitrarily Shaped Structures

2.1 Introduction

This chapter describes a novel method for determining the field distribution in a region of space comprising enclosed partly by surfaces with arbitrary geometries and material characteristics due to propagating electromagnetic waves. The instantaneous, spatially dependent, electric field is a vector sum of all the fields at the spatial location of interest. In principle, the time evolution of the field distribution at an arbitrary spatial location can be evaluated at discrete time intervals. The geometric method described here represents a rev-

olutionary departure from the currently accepted methods of computational electromagnetics, which provide a numeric solution to an assumed model. This departure is a significant step towards the development of design tools for the design of geometrical cavities or the like to achieve a prescribed field distribution pattern. These design tools rapidly provide a general direction to the determination of optimal geometries for achieving prescribed field distributions.

The thrust of the research being reported is the development of a methodology for the construction of realistic models for determining field distribution within geometrical cavities and the like with surfaces of various material characteristics. The method allows the determination of field distribution to any desired accuracy. As a result during the design phase one may start with very approximate distributions that can be used to determine general geometries and surface characteristics that would yield the desired field distributions. The geometries and surface characteristics can then be refined by moving into more accurate field distributions and incorporating their effects. For example, using the developed method one can design a cavity structure which has a highly asymmetric angular response to incoming radiation or another model might seek to produce a spatial null and isolation from the incoming radiation. The developed innovative method provides a time domain analysis, based on periodic functions, which is suitable for realistic causal systems and permits transient analysis of geometrical structures. The frequency response of the system can be obtained by a Fourier transform of the temporal response.

2.2 Method for the Design of Geometrically Shaped Structures for Achieving Prescribed Electromagnetic Field Distributions

Propagation of electromagnetic waves in any arbitrary media is characterized by Maxwells equations, and the constitutive relations. Particular solutions, subject to boundary conditions, are obtained using either analytic solutions or numerical techniques. These are well understood and numerous textbooks are available on the subject matter. It is not the intent to reproduce these methods here. It surmises to say that any electromagnetic field can be decomposed into a finite superposition of plane wave fields. The simplest electromagnetic wave is a transverse electromagnetic (TEM) plane wave, which propagates in free space at the speed of light c, with a characteristic wavelength λ and velocity v. In simple resonant structures, such as Fabry Perot, higher order modes exist in the structure and any one of those modes can generally be decomposed into a pair of counter-propagating plane waves. In a more general geometry, the solution space may comprise of both stable, localized resonant structures, as well as, unstable structures. The field distribution at a spatial location (x, y, z) at some time t_j, is a superposition of waves, originating from either multiple independent sources or multiple reflections or due to scattering. It is imperative to note the subtle difference in the use of "superposition", which is typically applied to determine the output response of linear systems when excited by an arbitrary input comprising of a harmonic expansion. Here, the superposition is applied to the outputs and no system linearity is assumed.

This formalism is extremely powerful as it allows for inclusion of non-linear effects, which are necessary to describe the response of geometrical singularities occurring at the sharp corners (90^o bends).

The research work reported in this thesis has applied this novel design approach to characterize the interaction of electromagnetic waves, particularly in the GHz regime, with geometric structures formed by shaping conducting and non-conducting surfaces. However, the methodology is applicable to broad classes of travelling waves interacting with physical structures. The effect of the shape and location of the surfaces for a required electric field distribution can also be assessed rapidly.

For example, this methodology can be used to design an effective system of gates/walls to protect harbor assets from storm damage. Another example could be in determining structures with geometric features which can be designed to have a unique geometric solution to provide a required electric field distribution so as to isolate sensitive electronics from a high field distribution broad band electromagnetic pulse (EMP).

In summary, my contribution to this work and the objective of the developed design tools is to determine a solution for the geometric features of a structure given a required distribution of the fields or radiation pattern. This is described as an inverse problem and is highly challenging because complex geometries have highly non-linear features which makes direct solution impossible and generally present more than one solution for the geometric features of a structure.

2.3 The Developed Method for Field Distribution Analysis and as a Design Tool

The fundamental concepts of the developed design method are discussed here through the use of a simple example of metallic (perfectly conducting) surfaces interacting with monochromatic waves, describing the scalar component of the electric field of the EM wave. A full time-varying response is obtained by determining the spatial response at discrete points of time, conforming to the fastest component in the system.

Consider the two-dimensional solution space, defined by a planar surface of finite extend as illustrated in Figure. 2.1. In the absence of any structure, a plane wave enters the solution space at $t = 0$. The electromagnetic plane wave varies sinusoidally in time and space and propagates in the Y direction. The electric field component of the incoming electromagnetic wave is considered to vary sinusoidally in the Z direction with a value of $+1$ volts per meter and -1 volts per meter. The incoming wave is assumed to be propagating in free space (ϵ_0), however, the method being described will accommodate any permittivity characteristics. The incoming wave can be considered a plane wave in the absence of any structure that enters the incidence path of the wave.

Now consider a finite planar surface that is positioned perpendicular to the XY plane as shown in Figure. 2.1. Then when the incoming wave interacts with this surface, it is reflected depending on the angle of incidence and the surface materials. Here the surface is considered to be metallic and perfectly conductive. The next step is to consider how the fields are distributed over the

surface at one instant of time. To this end, we lay a grid over the surface of the XY plane, thereby sub-dividing the space into small grid elements. The size of the grid elements must be smaller than the wavelength, preferably at most a quarter of the wavelength, so that we can examine each of the grid elements and determine the amount of charges distributed over the surface of the grid. The amount of charges distributed over a grid surface will be the combination of the amount of charges that are contributed by all electromagnetic waves that pass over the grid surface. The geometry of the incident wave is obviously sinusoidal, but may also be approximated by a step-wise pattern with the desired number of steps per period. The coarsest such approximation is a square wave and is used in the present example to describe the developed method. When the incident plane wave interacts with a surface, the surface geometry and material and the angle of incidence will determine how much of the incident field will be reflected off the wall and the direction of the reflected wave.

The process of determining the distributions of charges resulting from the incoming plane wave and its interactions with the surface of a surface such as the one shown in Figure. 2.1 at a given instant of time, the following steps are followed. Firstly, the interacting surface is removed and only the incident wave is considered. It is noted that if there are more than one incident wave is present, then each wave is similarly considered one at a time. From the magnitude of the electric field in each of the grid surfaces is determined (which could be determined as an average value or even more coarsely the closest value of the aforementioned square wave approximated incident wave). Next, the aforementioned surface, Figure. 2.1, is considered to be present and the amplitude

and direction of the reflected wave is determined based on the characteristics of the inserted surface. Once again, the distribution of the electric field over each grid element is similarly determined. It is again noted that if there are also more than one surface element, the reflections of each incident wave and their reflected waves over the surface of each grid element is similarly determined. Due to the linear characteristics of the present system, superposition is then used to add the contribution of each incident and reflected waves to the total electric field strength over the surface of each grid element. The distribution of the electric filed over the entire surface as bounded by the reflecting surfaces at the selected instant of time is thereby determined. A snapshot of the charge distribution over this surface at the selected instant of time is thereby obtained.

The next step is to determine how the charge distribution varies over time. To this end, the charge distributions over the aforementioned surface and inside the laid grid surfaces are determined over the desired length of time at small increments of time ΔT. The time increments ΔT must obviously be significantly smaller than half of period of the highest frequency electromagnetic incident wave considered. At each time interval, the above process is repeated and the distribution of electric field over the surface of each grid element id determined. For a steady state condition, the total length of time that needs to be covered is equal to the period of the wave with the longest wavelength. As a result, the time history of the field distribution over the aforementioned surface is determined and can be depicted in a manner similar to a video.

It is also noted that even though in the above description as well as in Figure. 2.1 a two-dimensional grid is shown to be used to discretize the XY

plane, the discretization is readily extended in the Z direction to obtain a three-dimensional grid within which the field distribution is similarly determined at each increment in time.

It is noted that by reducing the time intervals ΔT and by reducing the aforementioned grid size over the surface (space) to be studied, the accuracy of the obtained field distribution is increased. In fact as the time interval and the grid size tend to zero, the obtained field distribution tends to its actual analytically defined distribution. This shows the validity of the present approach for determining field distribution in arbitrarily shaped geometrical structures.

2.4 Example: Design of Geometrical Structures for a Prescribed Field Distribution

The following example is intended to clearly illustrate how the developed method can be applied to determine electric field distribution in arbitrary geometrical structures with any specified material characteristics. Initially we need to consider an arbitrary starting time, indicated here as time $t = 0$. The aforementioned snapshot of the status of the electromagnetic wave is then determined using the method described above. The starting phase of one of the incident waves at a specified spatial location is also used as reference at the above initial time of $t = 0$. In this example we also consider a two-dimensional solution space as was described for the example of Figure. 2.1, where a plane wave enters the solution space at $t = 0$. The electromagnetic plane wave prop-

agates in the Y direction. The incident electromagnetic wave is polarized with the electric field considered to in the Z direction with a value of $+/-1$ volts per meter. We will consider an incident wave that at the starting time $t = 0$ is at zero phase along the X axis, Figure. 2.2. The spatial grid used to discretize the space of wave propagation of interest is a quarter of wavelength in size and square in the XY plane as shown in Figure. 2.2. A fully conductive metallic surface is positioned perpendicular to the XY plane at 45 degrees angle as shown in Figure. 2.2. For the sake of simplicity, the wave is approximates as a square wave. The grid subdivides the space into squares in XY plane (cube in XYZ space) a quarter wavelength in size.

Following the present method, the first step is to remove the reflective surface, and lay the aforementioned grid over span of the XY plane to be considered as shown in Figure. 2.2. With the reflective surface removed, the distribution of the electric field (as approximated by a square wave) and at the time $t = 0$ at which the wave has a zero phase along the X axis is determined over the grid area. Noting that the square grids have a quarter of the wavelength size, the first two grids (in the Y axis direction) have an electric field amplitude of $+1$ volt, followed by two grids with an electric field amplitude of -1 volt as shown in Figure. 2.2. The pattern is repeated as shown in Figure. 2.2.

The next step is to place the finite sized reflective surface (with fully conductive surfaces) back as shown in Figure. 2.2, as shown to be oriented at 45 degrees with the incident wave. Considering no surface loss, the incident wave would have been reflected with the same angle with the normal to the surface as shown in Figure. 2.3, in this case parallel to the X axis. It is noted that

in Figure. 2.3 only the electric field generated by the reflected wave is shown. Here since the reflective surface is considered to be fully conductive, the wave would have been reflected with a reflection coefficient of negative one (-1). The reflected electromagnetic wave is re-transmitted from the point of interaction at the fully conductive metallic surface. The distribution of the electric field due to the latter re-transmitted electromagnetic field over the affected grid elements (parallel to the X axis) is similarly determined and is shown as indicated in the Figure. 2.3.

Now by superimposing the field distributions over the grid elements due to the incident wave as shown in Figure. 2.2 and due to the reflected wave as shown in Figure. 2.3, the electric field distribution over the selected surface area is determined as shown in Figure. 2.4. The resulting distribution clearly shows the effect of the fully conductive surface on the distributed field at the selected time $t = 0$. The process can then be repeated at small enough time intervals for a full period of the wave. As a result the time history of the electric field distribution over the selected surface area is determined. By reducing the size of the grids and by making a finer step-wise approximation of the electric field along the line of wave propagation, a finer resolution field distribution is obtained. If more than one incident wave is present (with the same wavelength or with different wave lengths) and/or if more than one reflective surface is present (with any material properties), their resulting electric field distributions are similarly determined (one by one) and their superposition provides a map of the electric field distribution over the selected surface area. It is also appreciated that the incident waves do not have to be polarized and if not polarized, the electric field variation along the travelled path at the selected

instant of time has to be included.

Figure. 2.5 shows an isometric view of the incident wave and the reflected wave shown in Figure. 2.4 at time $t = 0$ to more clearly show the process of determining the contribution of each to the resulting electric field distribution over the selected surface area. The approximated square wave incident and reflected waves ant the result of incident wave interaction with the fully conductive reflective surface is also clearly show. In this case, at the reflective surface if the incident wave has an amplitude of 1 volt/meter, than the reflected wave amplitude is seen to be -1 volt/meter. The change in the direction of the incident wave obviously follows the geometric law of reflection.

The time history of electric field distribution within the selected space is similarly determined by repeating the above process at small enough time intervals.

2.5 Summary

The present powerful method can be used to determine steady state as well as transient electric field distribution in any geometrical cavity constructed with arbitrarily shaped surfaces with different material characteristics when interacting with one or more polarized or non-polarized incident waves with fixed or varying amplitude and/or frequency. The method was shown to work for electromagnetic waves, but is is readily seen to work with almost any other wave types with any fixed or varying frequencies. The user must obviously note that spatial discretization must consider the wavelength of the shortest incident wave. The time increments between each field distribution snapshots

must also be considered to ensure that they are significantly smaller than half or even a quarter of the wave periods. The obtained field distributions and their time history may be determined with any accuracy by appropriately sizing the grid sizes and the time intervals. The method also can be seen to ready handle the presence of dielectric materials, even with spatially varying physical characteristics.

The method has the needed flexibility to easily define complex 3D surfaces by appropriate grid size selection. The 3D grid (voxel) elements may have fixed or varying geometries to accommodate the overall geometrical shapes and boundary conditions being considered. In the following chapter it is shown how the present method can be used to design geometrical structures to achieve a prescribed filed distribution with a selected space.

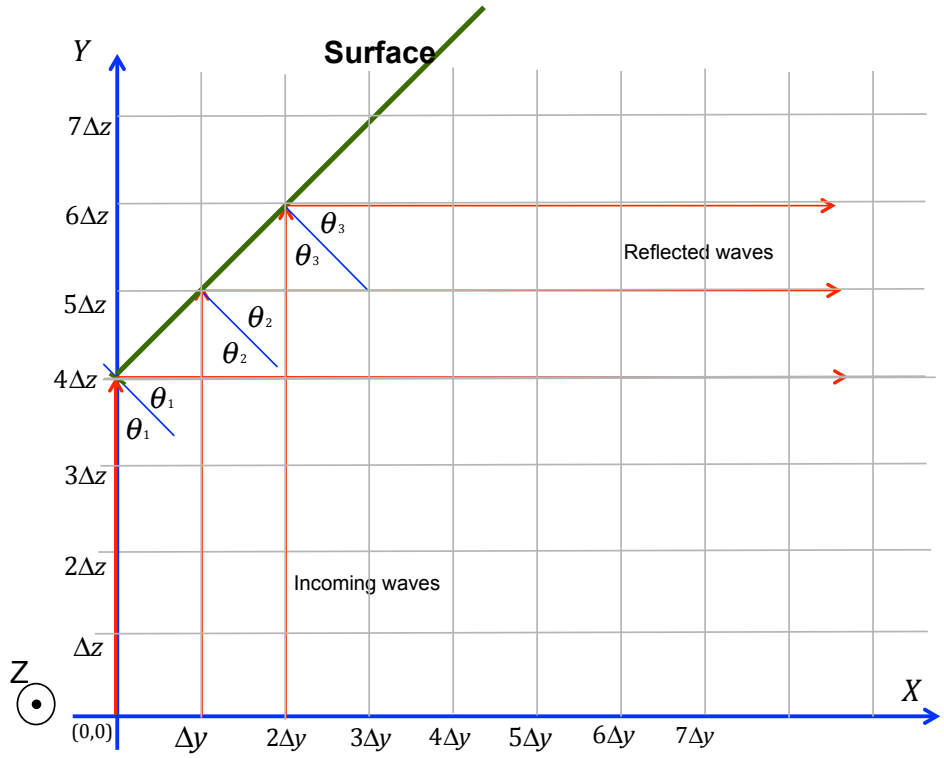

Figure 2.1: Two-dimensional solution space, defined by a planar surface of finite extend.

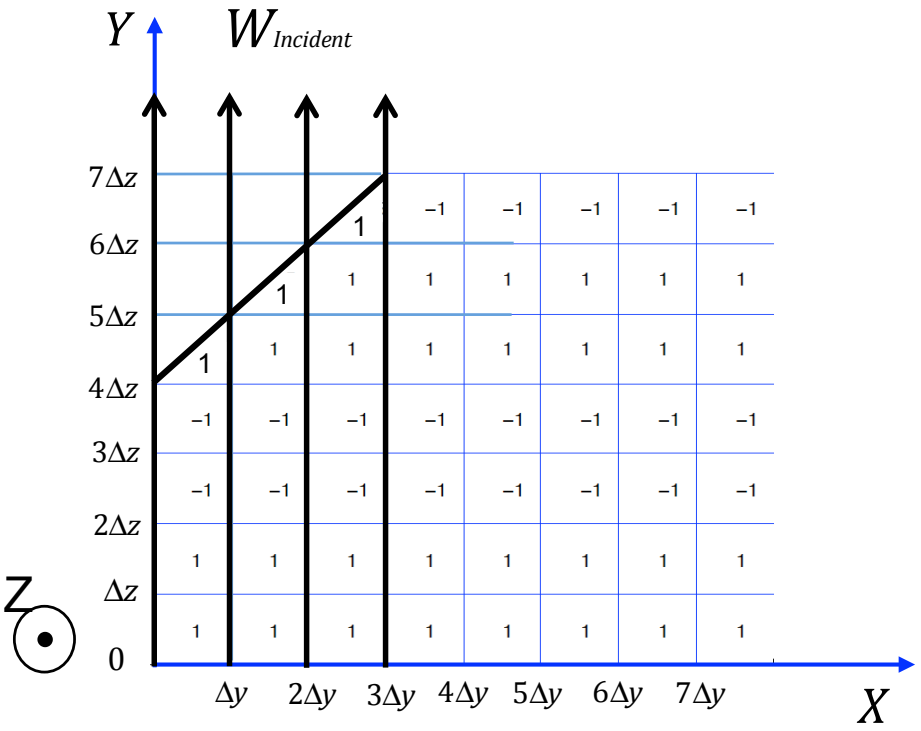

Figure 2.2: Incident wave starting at $t = 0$ with zero phase along the X-axis and a discretization grid of one quarter of the wavelength.

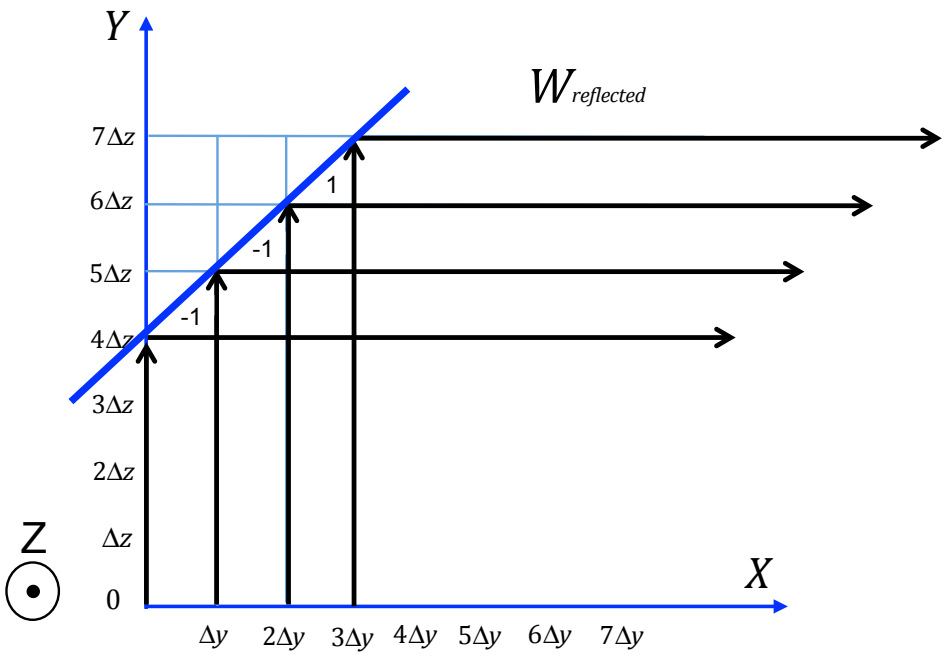

Figure 2.3: The electric field distribution at the time $t = 0$ due to the reflection of the incident wave.

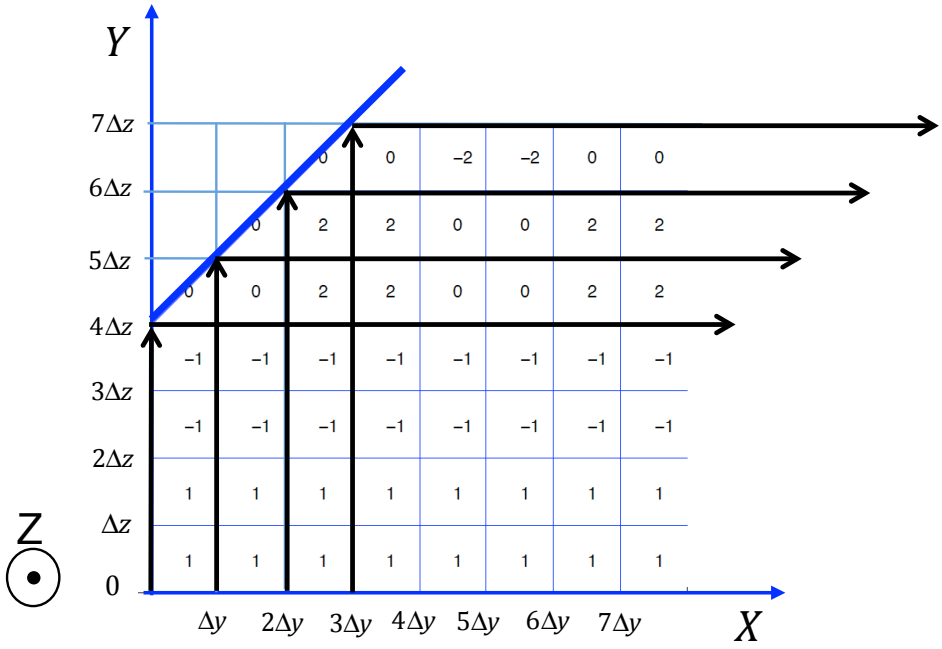

Figure 2.4: The distribution of the electric field due to the incident electromagnetic and its interaction with a conductive surface.

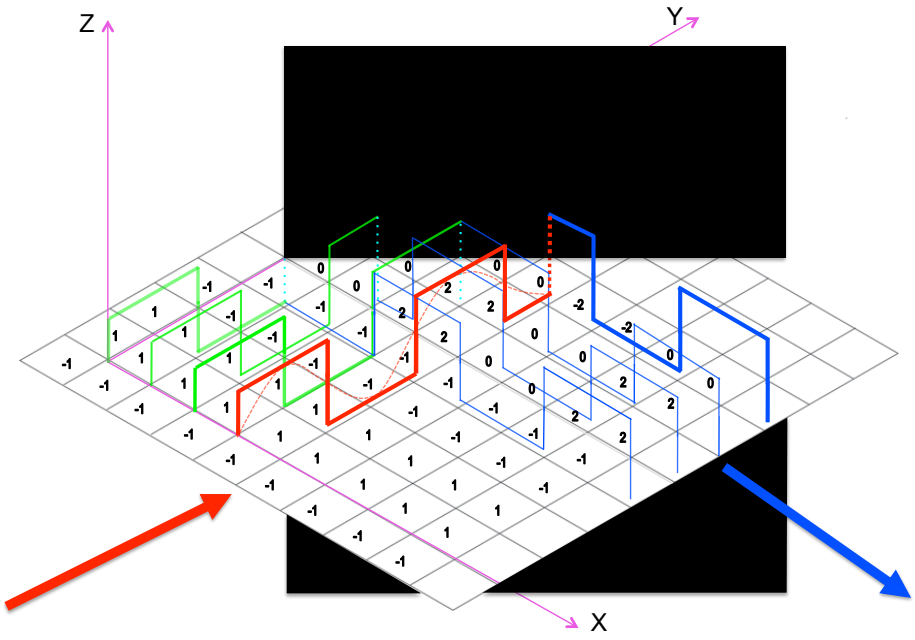

Figure 2.5: An isometric view of the distribution of the electric field due to the incident electromagnetic and its interaction with a conductive surface.

Chapter 3

Development of a Method to Design Geometrical Structures to Provide a Prescribed Electromagnetic Field Distribution

3.1 Introduction

This chapter illustrates the power of the design methodology described in the previous chapters by detailing the steps of the inverse problem through four diverse scenarios. In all examples, the sensor structure comprises of reflecting structures, orientated and positioned in free space. Further, the assumed structures are two dimensional and are illuminated by a plane wave source,

however, it is appreciated that the methodology is applicable to be multidimensional structures, which are illuminated by any arbitrary electromagnetic wave.

The objective of the inverse problem is to determine the location and orientation of the reflective surfaces, given the desired spatial distribution of the field. The four cases considered below are: 1) a localized region of high field strength; 2) a localized region of null field strength; 3) distributed regions of maximum filed strength; and 4) a localized region of minimal field strength. In all the examples considered, a spatial discretization of $\lambda/4$ is sufficient to demonstrate the methodology, while the source wavelength discretization of $\lambda/2$ will suffice.

To verify the efficacy of the methodology and the validity of the inverse solution obtained, a commercial finite element analysis high frequency electromagnetic solver, ANSYS, was used to compare the desired and analytical fields.

3.2 Case 1: A Localized spatial region of high field strength

The first case study uses the described method to determine the orientation and location of the reflectors so that the field distribution has a region of high field strength as sketched in Figure. 3.1 and indicated by the point $D1$. This condition requires that, at the location $D1$, the field contributions from incident, reflected or scattered waves must be in-phase, leading to constructive

addition.

A Cartesian co-ordinate system, as sketched in Figure. 3.1, is used to define the various components needed to describe the inverse problem. An incident electromagnetic wave propagates in the Y-direction with its amplitude variations in the negative Z-direction. As a result of the $\lambda/2$ discretization, two field values of positive one and negative one are allowed in any of the spatial pixels, as shown in Figure. 3.1. Furthermore the electromagnetic wave enters the sensor structure at $Y = 0$ and is considered to propagate in the Y-direction. As a result of this condition, all pixels along the X-axis have a value of one indicating that they are in phase. It should be noted that Figure. 3.1 is a snapshot of the electric field amplitude in the absence of any geometric structure. Here the binary discretization of the sinusoidal amplitude distribution leads to an approximate solution but adequately illustrates the functionality of the proposed method. While the use of a finer grid size will increase accuracy, the increased the computation time limits the ease with which design trends can be readily explored by rapidly manipulating the model geometry.

However, it should be noted that the above discretization of space and time leads to solutions which approach the true solution in the limit of infinitesimally small step size.

With reference to Figure. 3.2, a proposed solution to this case study, comprises of a pair reflecting surfaces $S1$ and $S2$ which receive the incident electromagnetic wave and reflected radiated fields that contribute to the average field intensity at location $D1$. The sequence of Figures. 3.2 through Figures. 3.4 highlight the individual components of the net field amplitude in the spatial region $D1$. Figure. 3.2 shows the reflected field contributions from surface $S1$

at location $D1$ and Figure. 3.3 shows the contribution from a selected surface $S2$. The net field amplitude arising from the superposition of the contributions from surfaces $S1$, $S2$, and the incident field for is sketched in Figure. 3.4. The spatial distribution is a snapshot of the field amplitude, corresponding to a particular a phase of the propagating incident EM plane wave. Subsequently a temporal variation of the spatial field distribution is constructed by taking multiple snap shots at different phase points of the incident plane wave.

In summary, the interaction of the incident electromagnetic wave with surfaces $S1$ and $S2$ produces the desired high field distribution in the spatial region $D1$. One possible solution is characterized by the two reflecting surfaces orientated at 45^o and positioned as indicated in Figure. 3.2.

The efficacy of the design is established by obtaining a numerical solution of the electric field amplitude for the particular sensor design obtained using the new methodology. As discussed in Chapter 1 several numerical techniques for determining the electric field amplitude for arbitrary structures are available. Of these the ANSYS MultiPhysics finite element analysis software is used in this thesis. The model is created using ANSYS APDL environment and the high frequency EM solver is used to extract the vector solution of the spatial distribution of the electric field. Figure. 3.5 is a cross-sectional view of the geometric model. The sensor volume includes the two reflecting surfaces, labeled $S1$ and $S2$, corresponding to surfaces $D1$ and $D2$ referenced in the above discussion. The sensor volume is surrounded by a volume defined as a computational domain, which defines the complete solution space. The computational domain is surrounded by a perfectly matched layer (PML) to absorb all the incident EM wave, preventing unwanted reflections from enter-

ing the computational space. The surface S1 is defined by a planar surface passing through points $(0, \lambda, 0)$ and $(0.5\lambda, 1.5\lambda, 0)$. The surface $S2$ is defined by a planar surface passing through points $(3\lambda, \lambda, 0)$ and $(3.5\lambda, 1.5\lambda, 0)$. Figure. 3.6 is a vector of the electric field in the computational volume. The phase of the incident plane was adjusted to be the same as that used in the inverse method described above. The region enclosed by the squared corresponds to the spatial region $D1$ where the electric field amplitude is high. There is high correlation between the numerical results and the desired response, indicating that the sensor, designed using the methodology described here, is a viable inverse solution.

3.3 Case 2: A Localized null region of field strength

A second examples seeks to find a sensor structures that produces a localized a null spatial region. In other words, the inverse problem can be stated as, find a geometric structure that provides isolation from the incident electric field without the use of a conductive enclosure. With reference to Figure. 3.7 the particular null region is labeled as D2. All other pixels are filled with numeric values corresponding to the discretized incident plane wave in the absence of any structures within the computational volume.

The conceptual approach to the inverse problem dictates that an additional planar surface needs to be added to the sensor model developed for Case 1. As described above, the inverse problem is solved by breaking down the problem

into it independent fields arising from each of the surfaces and adjusting the surface location and orientation that leads to the desired net field distribution in the localized area $D2$.

Solution to the inverse problem begins by considering two perfectly conducting surfaces $S1$ and $S2$ orientated at 45^o and -45^o. The surface $S1$ is defined by a plane passing through points $(0.5\lambda, \lambda, 0)$ and $(\lambda, 1.5\lambda, 0)$. The surface S2 is defined by a plane passing through points $(3\lambda, \lambda, 0)$ and $(3.5\lambda, 1.5\lambda, 0)$. Figure. 3.8 and Figure. 3.9, show the corresponding field amplitudes from $S1$ alone and $S2$ alone, respectively. The resultant field from the superposition of reflected waves from the two surfaces $S1$ and $S2$ produces a null in the spatial region $D2$ as illustrated in Figure. 3.10. However, when the incident filed is included in the summation, the net field amplitude in region $D2$ in longer zero as shown in Figure. 3.11.

It is clear that an additional conducting surface is required to null out the field in the spatial region $D2$. One possible location of the reflective surface $S3$ is determined by requiring that the field due to $S3$ alone should have an amplitude of -1 in the spatial region of interest $D2$. As illustrated in Figure. 3.12 the surface $S3$ has an orientation angle of 0^o and is defined by a plane passing through points $(1.5\lambda, 2\lambda, 0)$ and $(2\lambda, 2\lambda, 0)$. Figure. 3.13 shows a solution to the inverse problem of case 2, comprising of three reflecting surfaces with the given orientation and location. The net electric field arising from the superposition of the incident and reflected waves leads to a null in the spatial region $D2$.

As in Case 1, the efficacy of the designed sensor geometry is assessed by comparing the expected field distribution in region $D2$ with that computed us-

ing ANSYS. Figure. 3.14 is the generated geometric model for ANSYS simulation. Figure. 3.15 shows the vector plot of the electric field in the computation volume. A spatial region $D2$, indicated by the square outline, clearly shows that the net electric field is zero. It should be noted that ANSYS simulation has been performed with an element size of $\lambda/20$.

3.4 Case 3: Distributed spatial regions of high field strength

This particular inverse problem seeks to find a sensor geometry that results in distributed regions of space with the required field strength. In this particular example, a maximum electric field amplitude is required in two distinct spatial regions labeled $D3$ in Figure. 3.16. Following the above described method for solving the inverse problem, the contribution of each reflecting surface is considered separately and as pairs, until the desired field amplitude is obtained in the designated spatial regions.

Figure. 3.17 shows the field amplitude corresponding to a single reflector $S1$, orientated at 45^o defined by a plane passing through points $(0, \lambda, 0)$ and $(0.5\lambda, 1.5\lambda, 0)$. Figure. 3.18 shows the field amplitude corresponding to a single reflector $S2$, orientated at -45^o defined by a plane passing through points $(3\lambda, 1.5\lambda, 0)$ and $(3.5\lambda, \lambda, 0)$. Figure. 3.19 is the field amplitude distribution due to $S1$ in the presence of $S2$. Figure. 3.20 is the resultant field amplitude distribution from reflections arising from both $S1$ and $S2$. Since the design requires a resultant field amplitude greater four times the initial amplitude

additional reflecting surfaces are needed to obtain the perquisite amplitude in the regions $D3$.

Figure. 3.21 shows the field amplitude corresponding to a single reflector $S3$, orientated at 45^o defined by a plane passing through points $(0.5\lambda, 2\lambda, 0)$ and $(\lambda, 2.5\lambda, 0)$. Figure. 3.22 shows the field amplitude corresponding to a single reflector $S4$, orientated at -45^o defined by a plane passing through points $(1.5\lambda, 1.5\lambda, 0)$ and $(2\lambda, 2\lambda, 0)$. Figure. 3.23 is the field amplitude distribution due to $S3$ in the presence of $S4$. Figure. 3.24 is the resultant field amplitude distribution from reflections arising from all four reflecting surfaces.

The net electric field arising from the superposition of the incident and reflected waves leads to a net electric field amplitude 4 in the two spatially distinct regions $D3$ as illustrated in Figure. 3.25.

The efficacy of the designed sensor geometry of Case 3 is assessed by comparing the expected field distribution in regions $D3$ with that computed using ANSYS. Figure. 3.26 is the generated geometric model for ANSYS simulation. Figure. 3.27 shows the resultant vector plot of the electric field in the computation volume. The two distinct regions $D3$ of high field amplitude are clearly visible and in very good agreement with the initial definition of the inverse problem.

3.5 Case 4: A Localized null region of field strength with multiple surfaces

This example is similar to Case 1, but seeks a design solution based on multiple reflecting surfaces, resulting in sharper transition between nearest neighboring pixels. In this particular example, a null in the electric field amplitude is required in a localized spatial region labeled $D4$ in Figure. 3.28. Figure. 3.29 shows the field amplitude corresponding to a single reflector $S1$, orientated at 0o defined by a plane parallel to $X = 0.75\lambda$, in the presence of a second reflector $S2$, orientated at -45^o defined by a plane passing through points $(2.5\lambda, 1.5\lambda, 0)$ and $(3.25\lambda, 0.75\lambda, 0)$. It should be noted that for consistency of the boundary conditions at the reflective surface amplitude of the reflected amplitude is -1. Figure. 3.30 is the field amplitude distribution due to $S2$ in the presence of $S1$. Figure. 3.31 is the resultant field amplitude distribution from reflections arising from both $S1$ and $S2$. Figure. 3.32 shows the field amplitude corresponding to a single reflector $S3$, orientated at 45^o defined by a plane passing through points $(\lambda, 1.75\lambda, 0)$ and $(1.25\lambda, 2.0\lambda, 0)$. Figure. 3.22 shows the field amplitude corresponding to a single reflector $S4$, orientated at -45^o defined by a plane passing through points $(1.5\lambda, 1.75\lambda, 0)$ and $(2\lambda, 2\lambda, 0)$. Figure. 3.33 is the resultant field amplitude distribution from reflections arising from all four reflecting surfaces. However, as the net field amplitude in region $D4$ is 1, a surface $S5$ needs to be added to the geometry as illustrated in Figure. 3.34. Figure. 3.35 shows the net electric field arising from the superposition of the incident and reflected waves from all five surfaces. The spatial

region $D4$ shows a null in the electric field. It should be noted that null region extends along the X-axis, including region $D4$.

The efficacy of the designed sensor geometry of Case 4 is assessed by comparing the expected field distribution in regions $D4$ with that computed using ANSYS. Figure. 3.36 is the generated geometric model for ANSYS simulation. Figure. 3.37 shows the resultant vector plot of the electric field in the computation volume. The required null in the electric field in region $D4$, enclosed by a square, is obtained, confirming the validity of the designed sensor. However, in this case there is a better null field match at other locations along the X-axis.

This discrepancy indicates that manual placement of the mirror surfaces is a challenging problem, which becomes more acute with increasing number of reflecting surfaces. Each surfaces, in the 2-D geometry, has three degrees of freedom, reducing the probability of finding the best design solution through this manual process. Thus, in these situations an iterative process of design and analysis is needed to reduce the number of possible design solutions. For example, in this case a second iteration may be performed using smaller $S1$ and $S2$ reflecting surfaces, which will certainly remove the unwanted high field regions labeled $R1$ and $R2$.

3.6 Summary

In the above analysis four distinct case studies have been presented to demonstrate the utility of the design methodology described in this thesis. For each of the four cases the designer is presented with the target spatial distribution

of the electric field to be achieved within a solution space. In all cases discussed, the inverse problem is simplified by constraining the sensor structure to be made from distributed, perfectly reflective planar surfaces, whose orientation and location are to be determined. In addition, the sensor is illuminated with a plane wave, which is linearly polarized in the z-direction. Solution to the inverse problem, i.e., design of a particular sensor, is based on the a priori knowledge of the interaction of the EM wave with the reflective surfaces. For example, in the above discussed cases, the tangential (Z-component) of the electric field has been assumed, leading to the surface boundary condition which requires that the net tangential electric field be zero at the surface. Under these simplifying assumptions, which have been imposed solely for the purpose of mathematical convenience, it has been possible to extract the inverse solutions for all four cases presented above. Additionally,spatial discretization of $(\lambda/4)$, used in solving the inverse problem, is sufficient as there is very good agreement between target field distribution and that computed from the design model using commercial software.

It can be appreciated from the special cases presented above that the method of obtaining a sensor design to achieve a given filed distribution has very broad applicability, as it is based on the fundamental concept of superposition. The net field at any spatial location is a vector sum of the electric fields arising from multiple sources, such as specular or diffuse reflective surfaces or localized scattering centers. A full 3-D mapping of the electric field can be constructed with the aid of specially developed software tools. A tool kit comprising of different types of scattering surfaces and/or scattering volume elements can be developed to describe the relationship between the incident

and reflected (or scattered) electric field. The designer would access the various tools, position and orient them according to developed guidelines and compute the electric field distribution map. Furthermore, due to relative low computational demand, the design tool can be interactive, so that the designer can rapidly visualize the effects of particular scattering elements, by just dragging and orienting them in real time. In this way the inverse problem can be iteratively solved in real time, resulting in considerable cost saving.

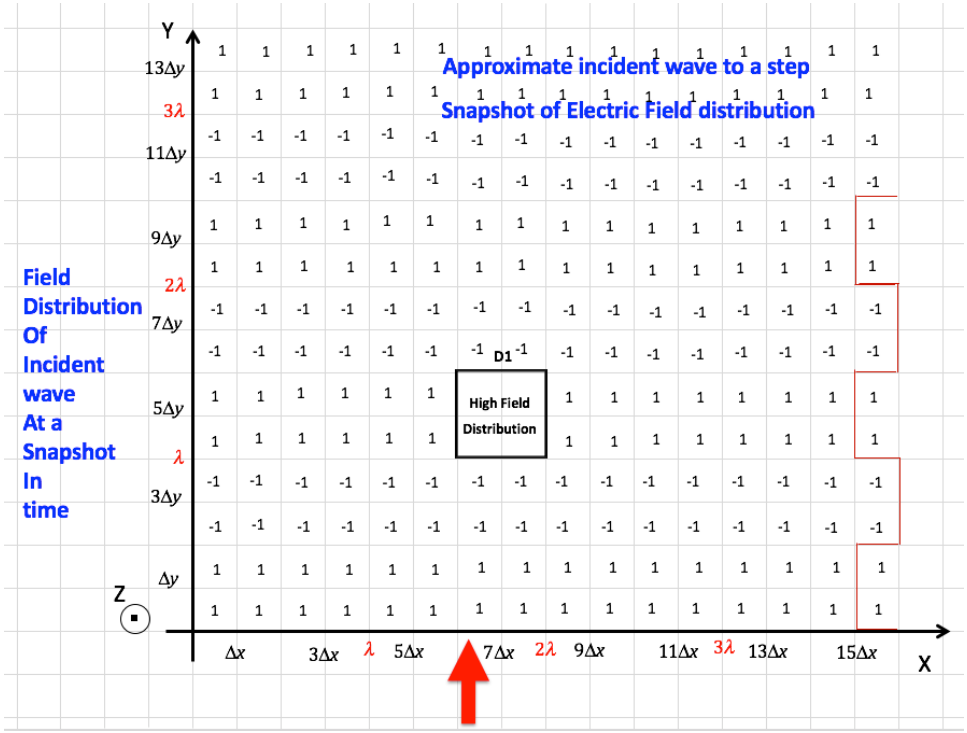

Figure 3.1: Spatial distribution of electric field due to incident plane wave. Incident wave propagates in the X-direction and its positive peak electric field amplitude is in the positive X-direction. Its negative peak electric field amplitude is in the $-X$-direction.

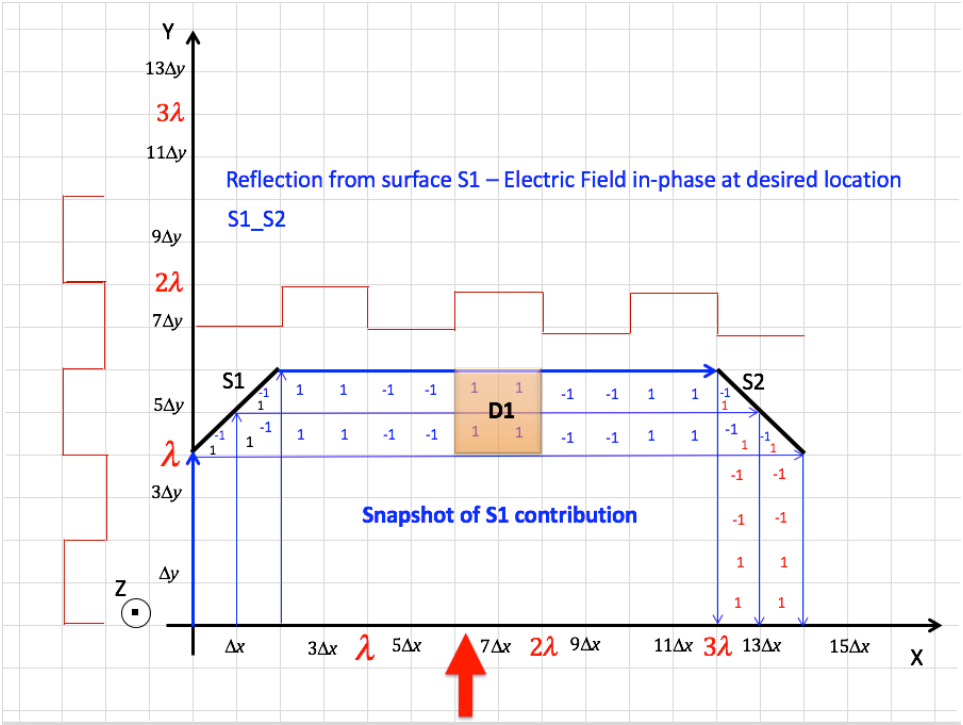

Figure 3.2: Surfaces $S1$ and $S2$ contributions to the electric field intensity at $D1$.

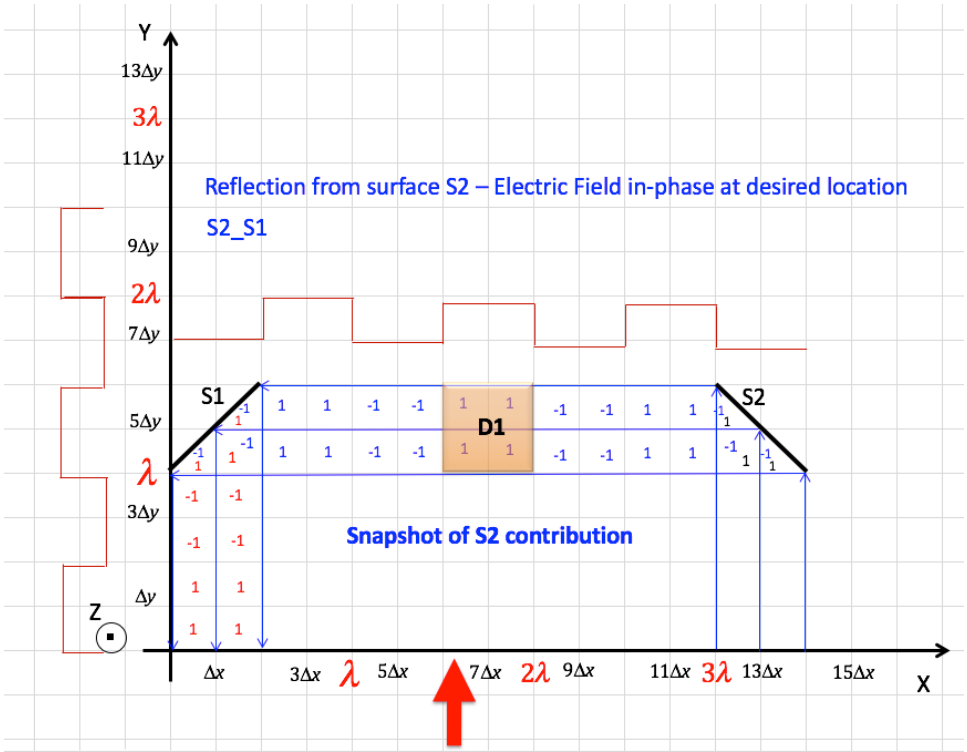

Figure 3.3: Surfaces $S2$ and $S1$ contributions to the electric field intensity at $D1$.

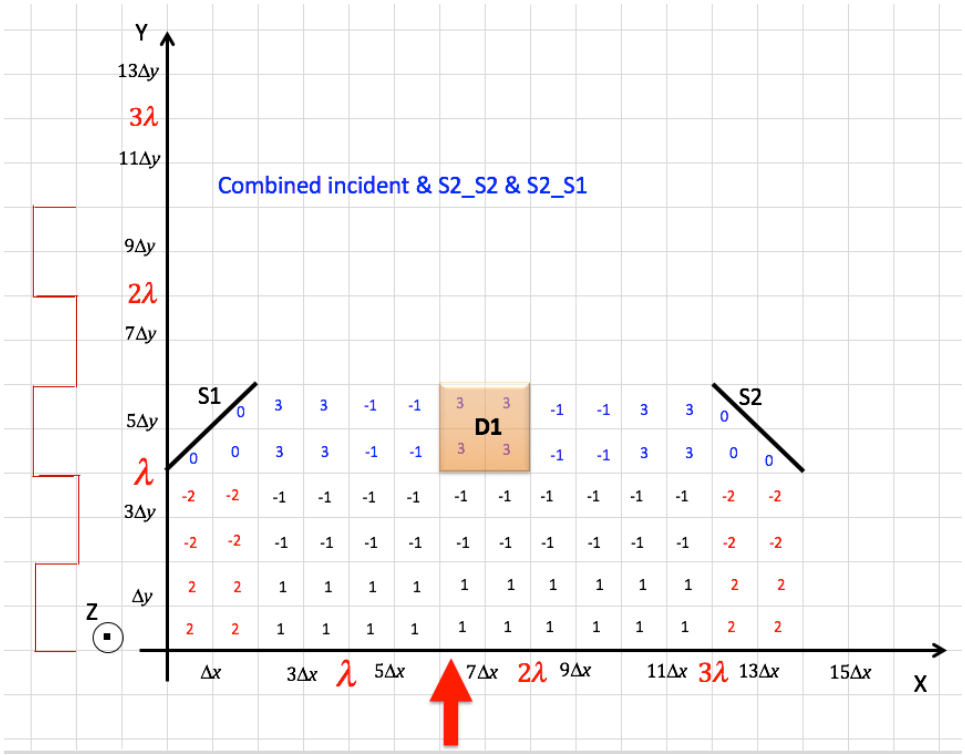

Figure 3.4: Snapshot of contributions of $S1 - S2, S2 - S1$ and the incident electromagnetic wave.

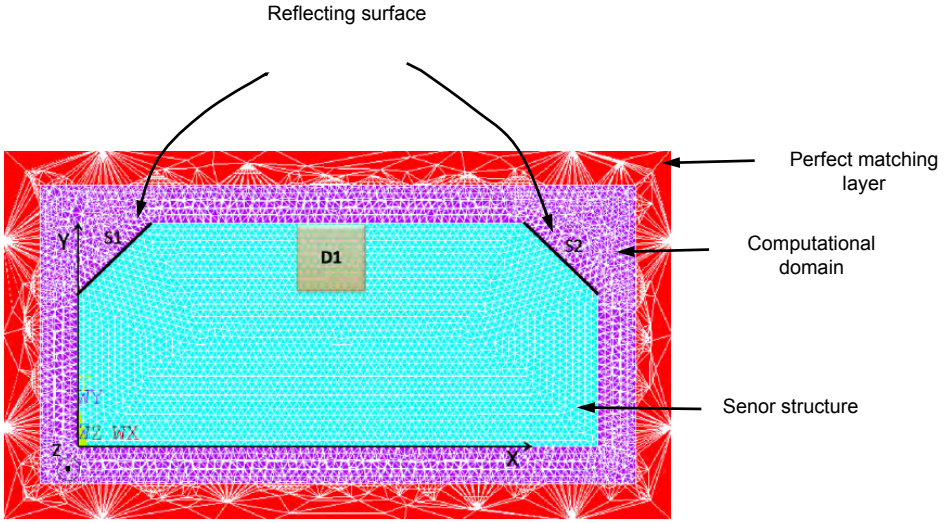

Figure 3.5: ANSYS analysis.

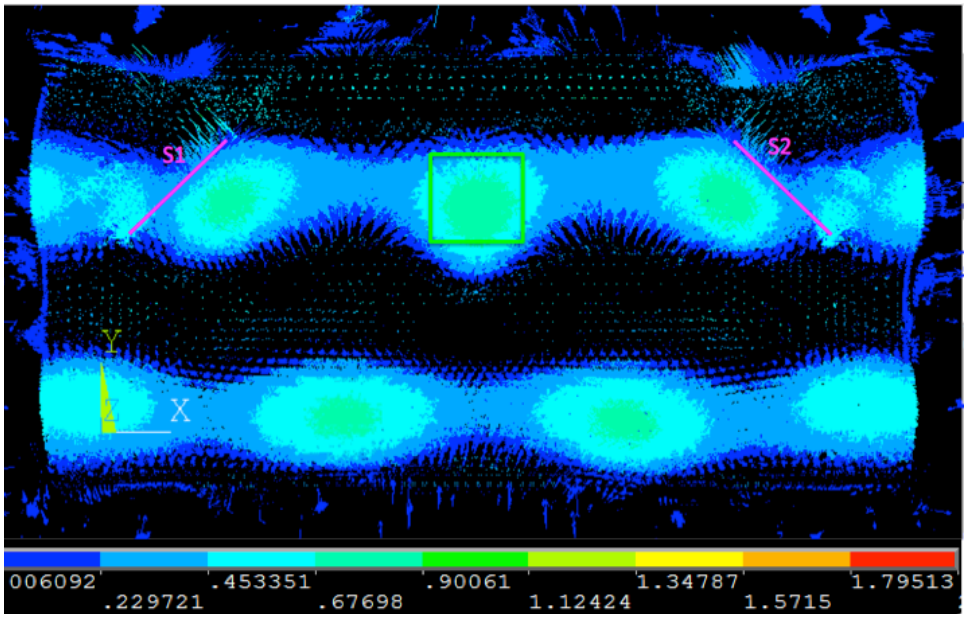

Figure 3.6: Vector plot of the electric field obtained using ANSYS for the geometry of Figure. 3.5).

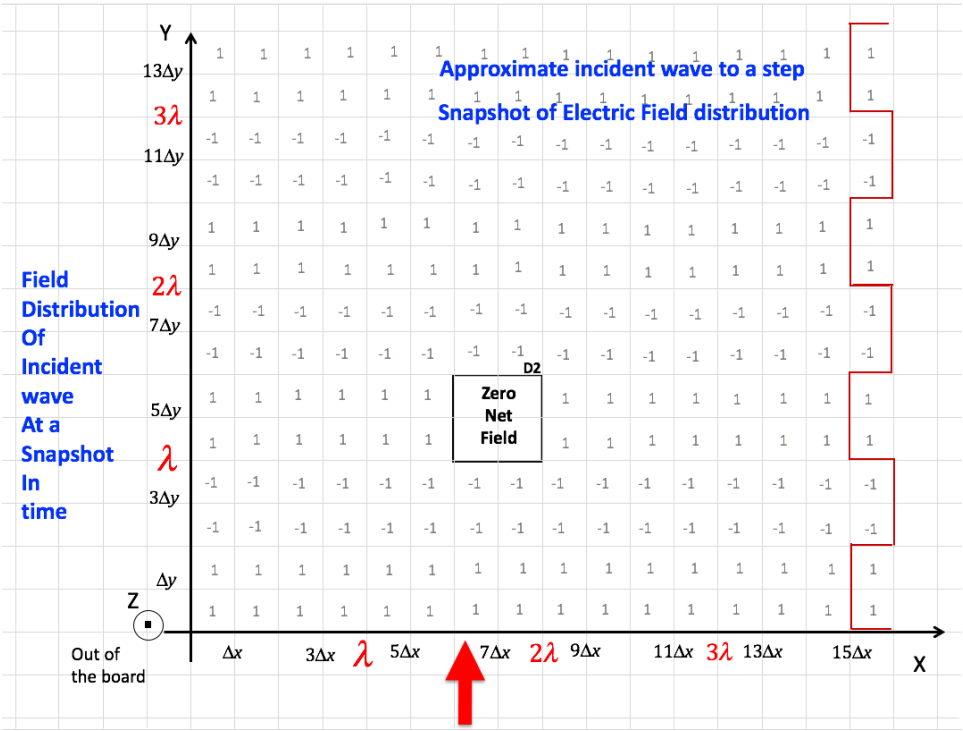

Figure 3.7: Example 2, desired field distribution $D2$.

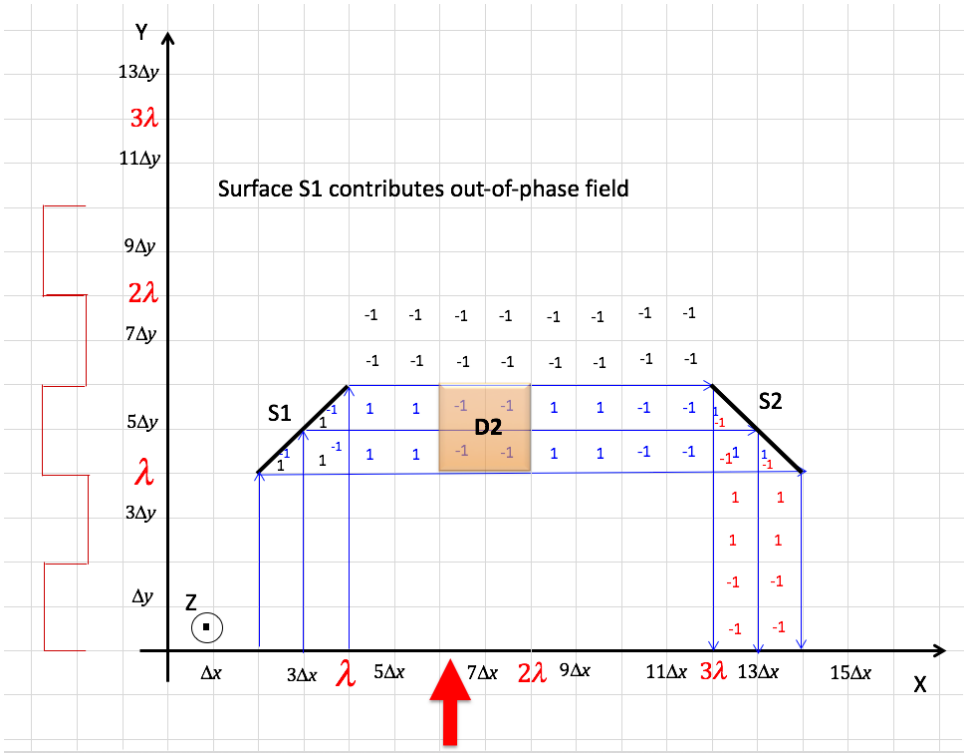

Figure 3.8: Contribution of surface $S1$.

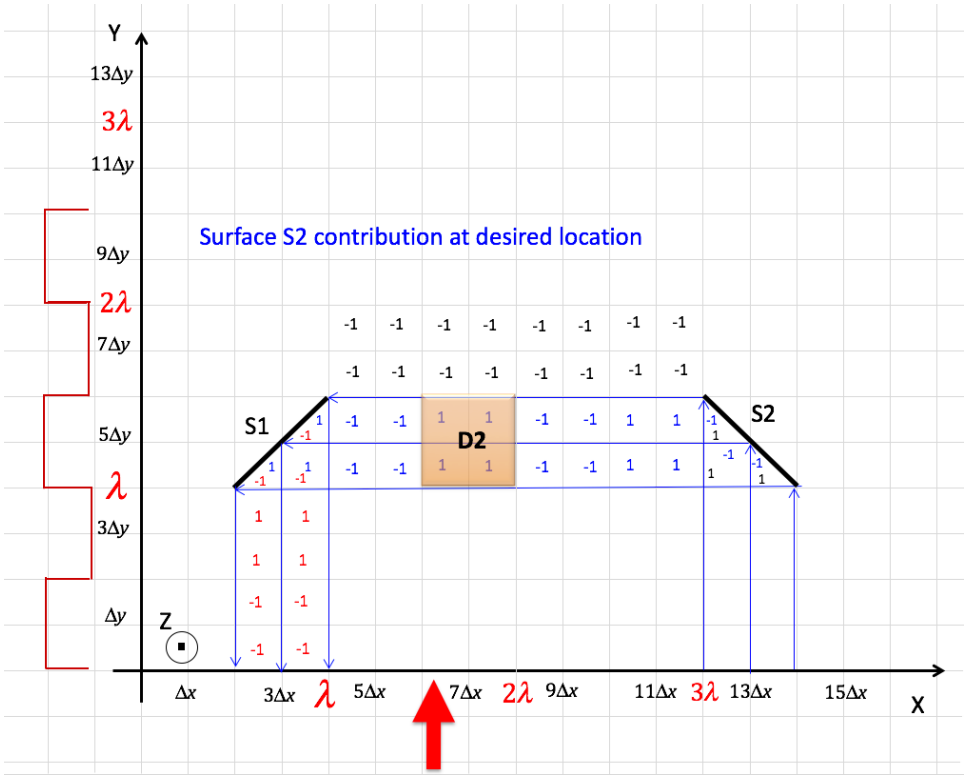

Figure 3.9: Contribution of surface $S2$.

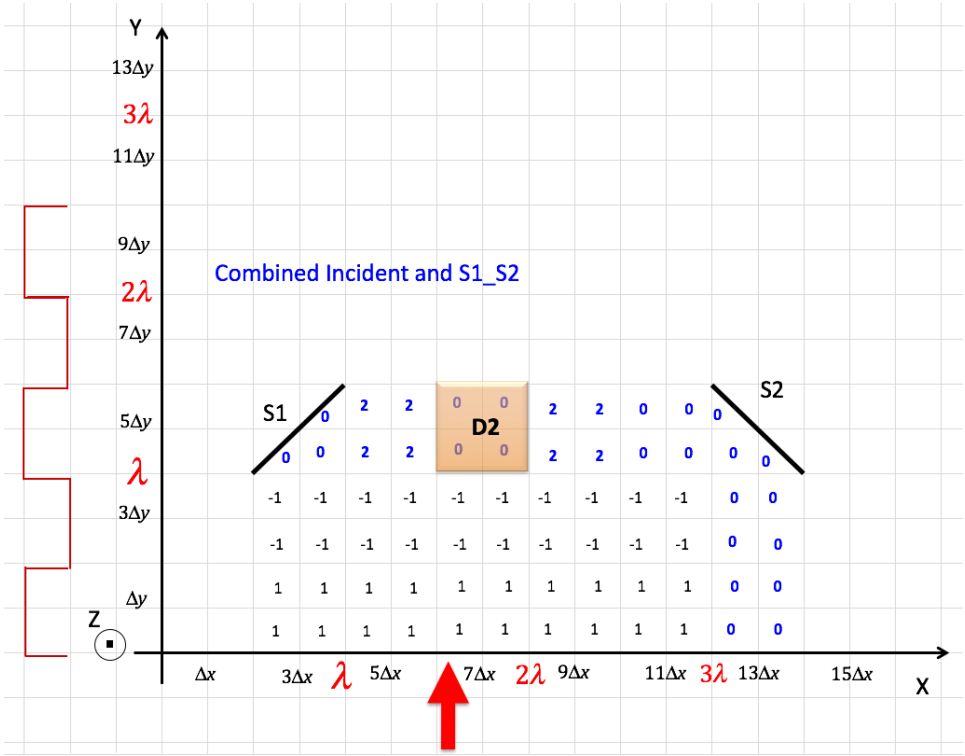

Figure 3.10: Incident wave combined with $S1$ and $S2$.

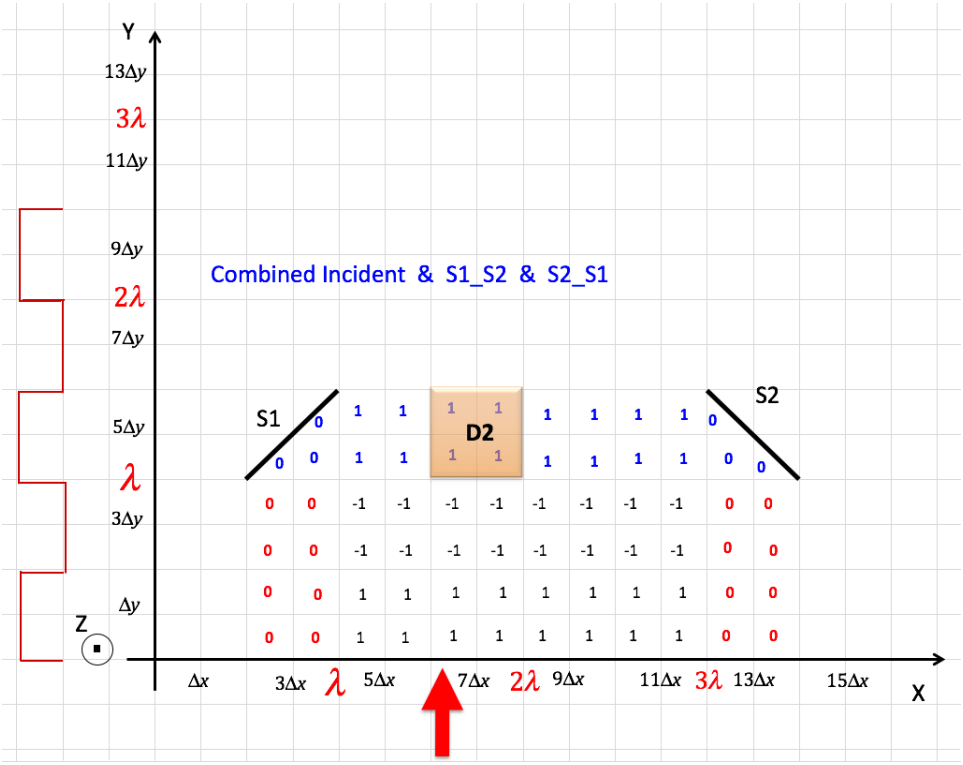

Figure 3.11: Combined average spatial field distributions for $S1, S2$ and the incident electromagnetic wave.

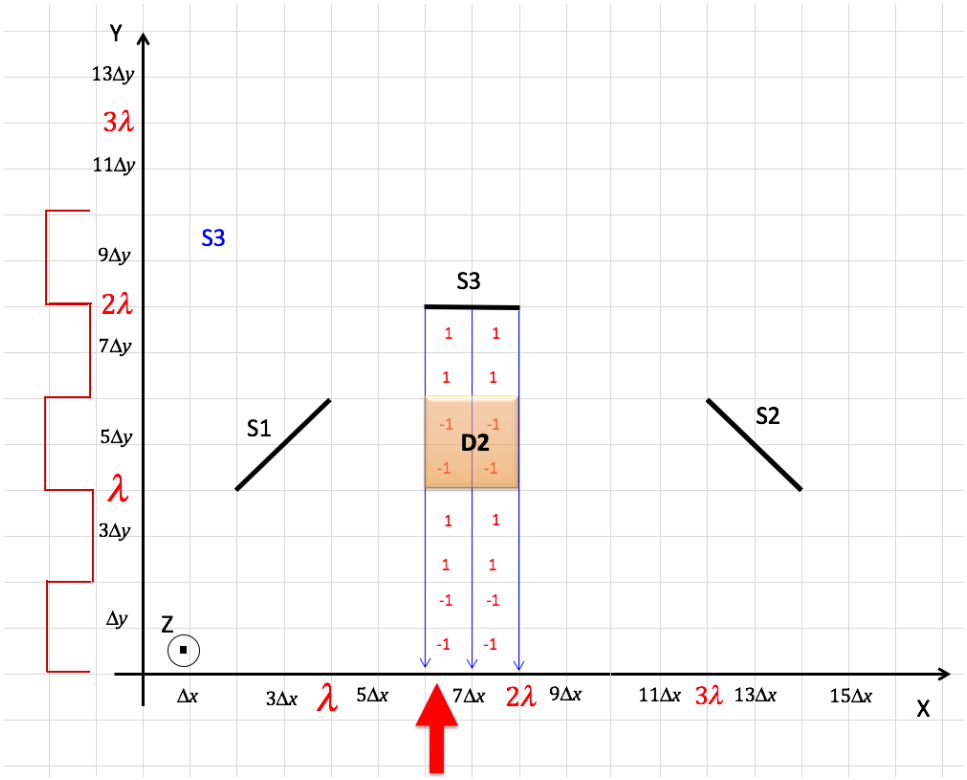

Figure 3.12: Average spatial field distribution for surface $S3$.

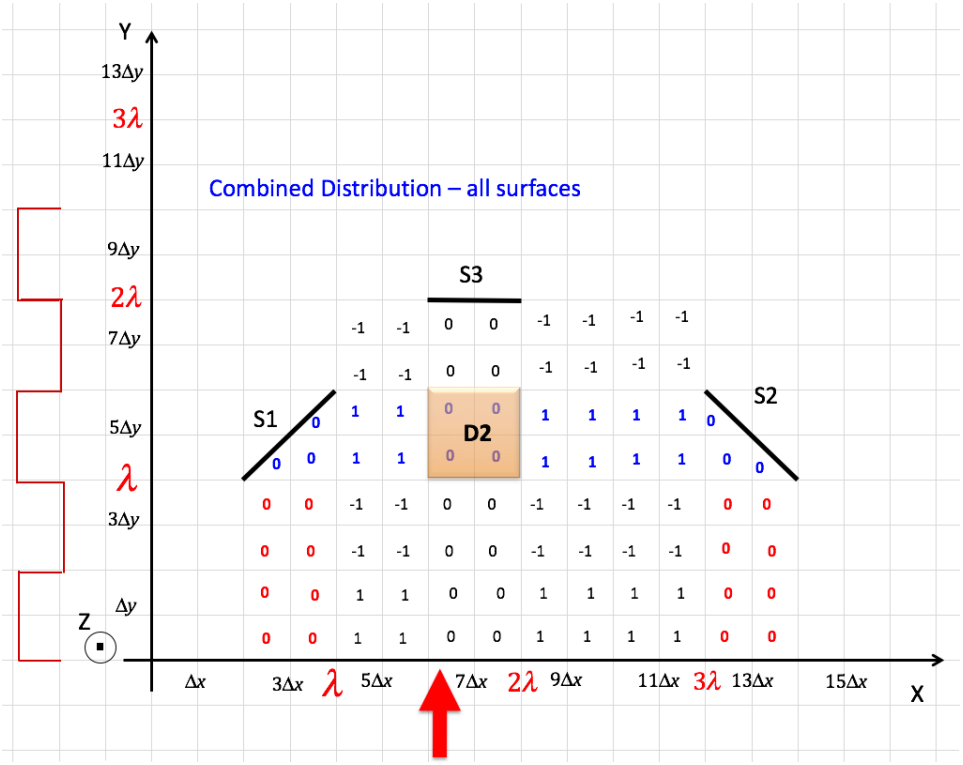

Figure 3.13: Average spatial field distribution for all surfaces combined and incident wave.

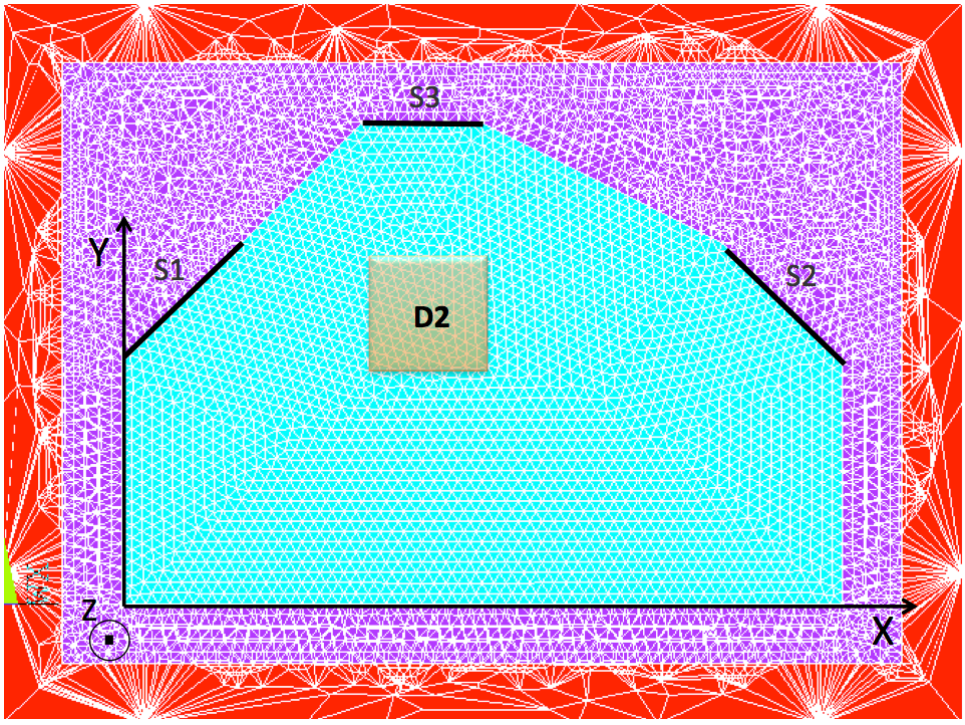

Figure 3.14: ANSYS mesh with a spatial discretization of lambda divide by 20. Surfaces $S1, S2, S3$.

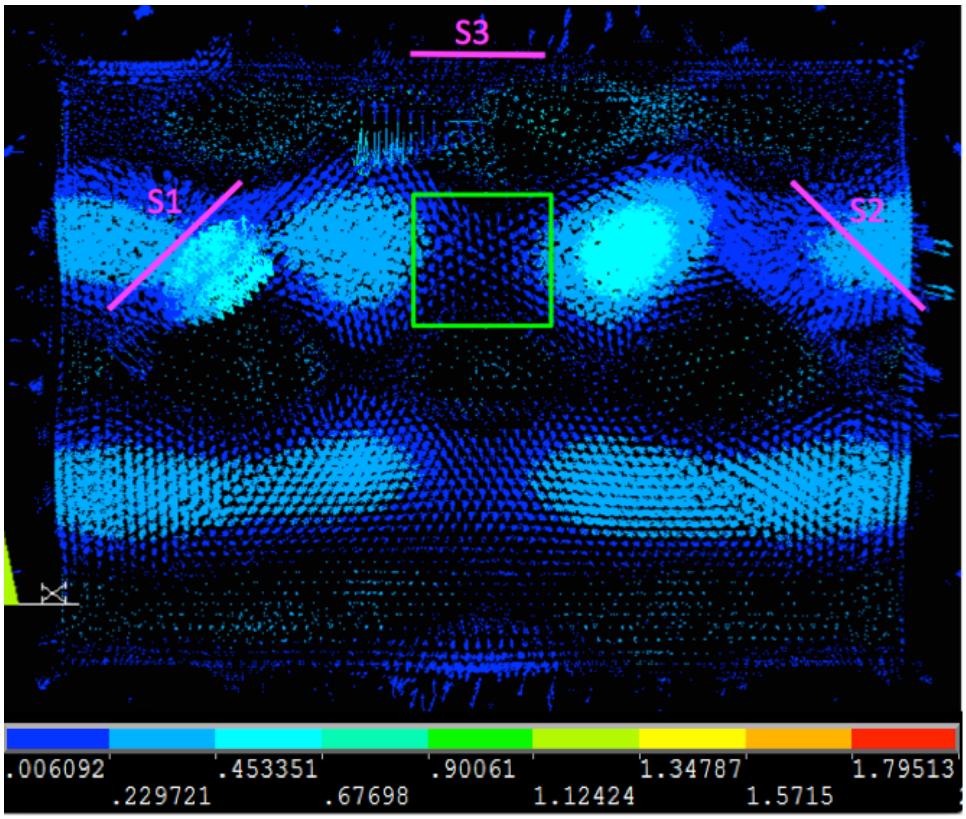

Figure 3.15: Results from the simulation analysis clearly show that the design method being reported strongly match the results from the ANSYS simulation analysis.

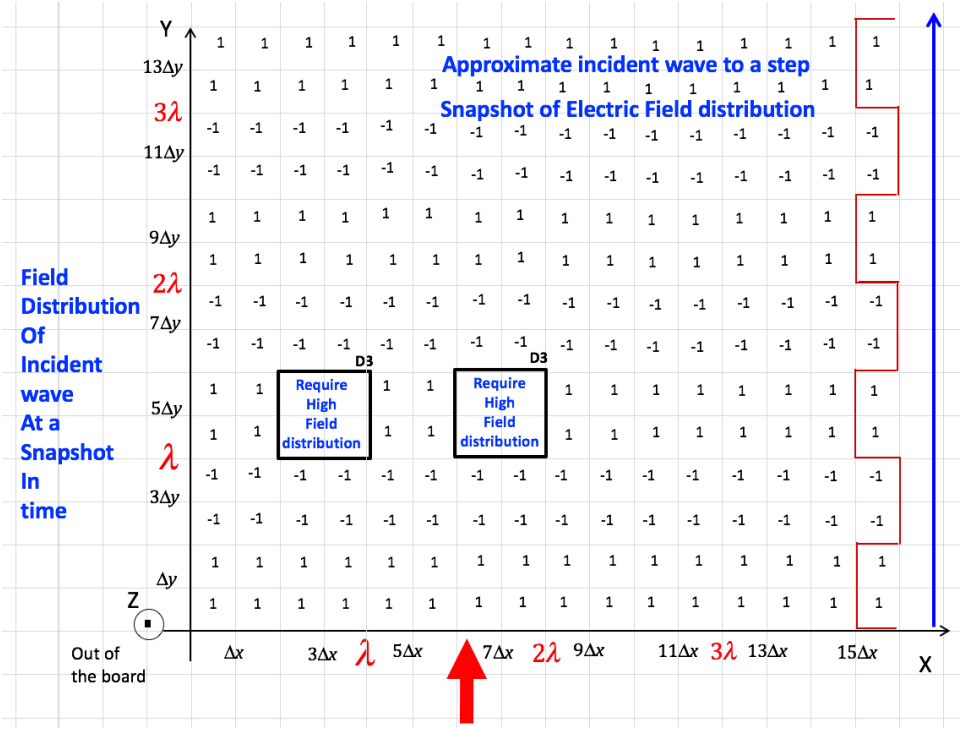

Figure 3.16: In example 3 it is desired to have two high energy regions at $D3$ locations.

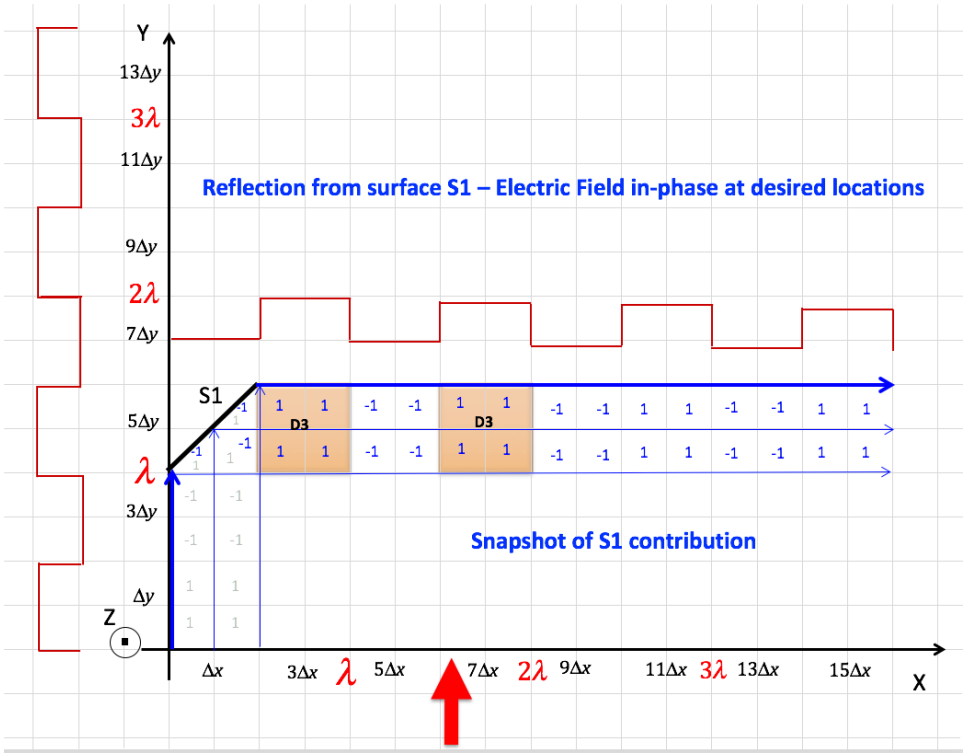

Figure 3.17: Contribution of surface $S1$.

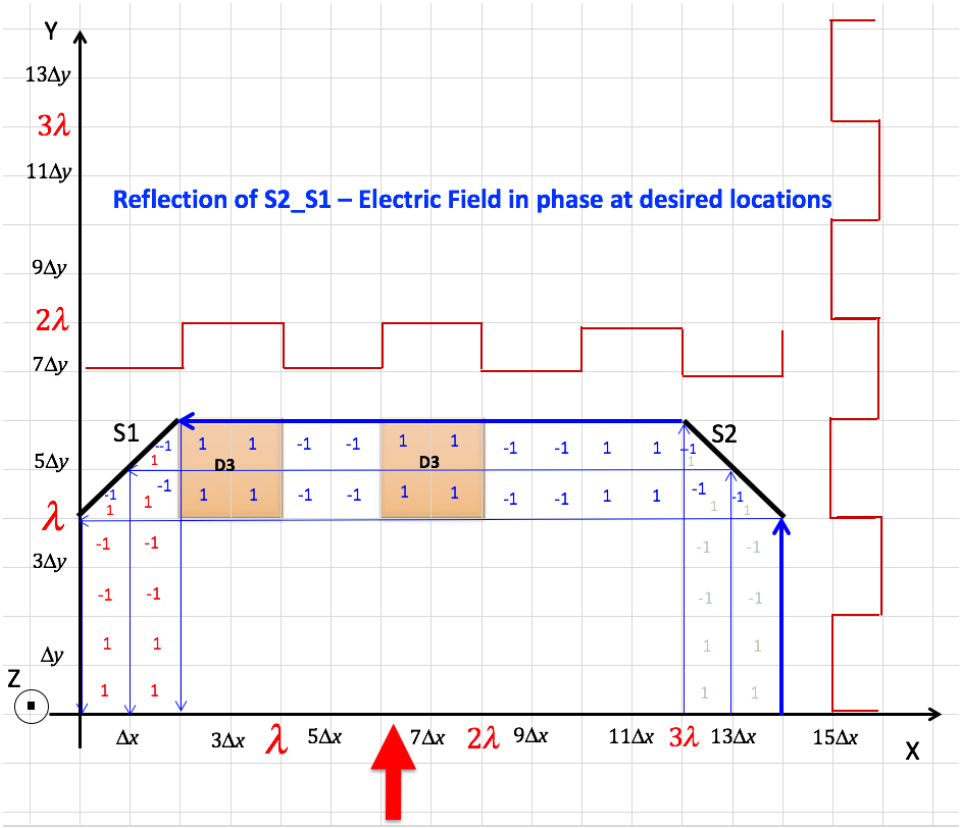

Figure 3.18: Fields reflected from surface $S2$ are in phase at desired locations.

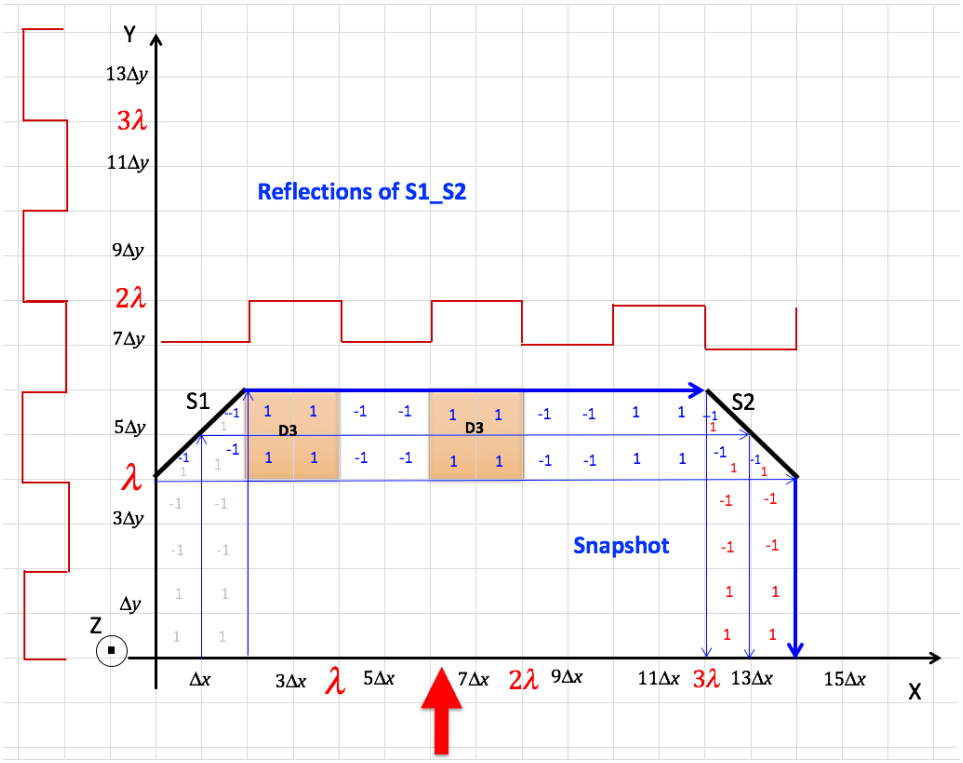

Figure 3.19: Fields reflected from surface $S2$ are in phase at desired locations.

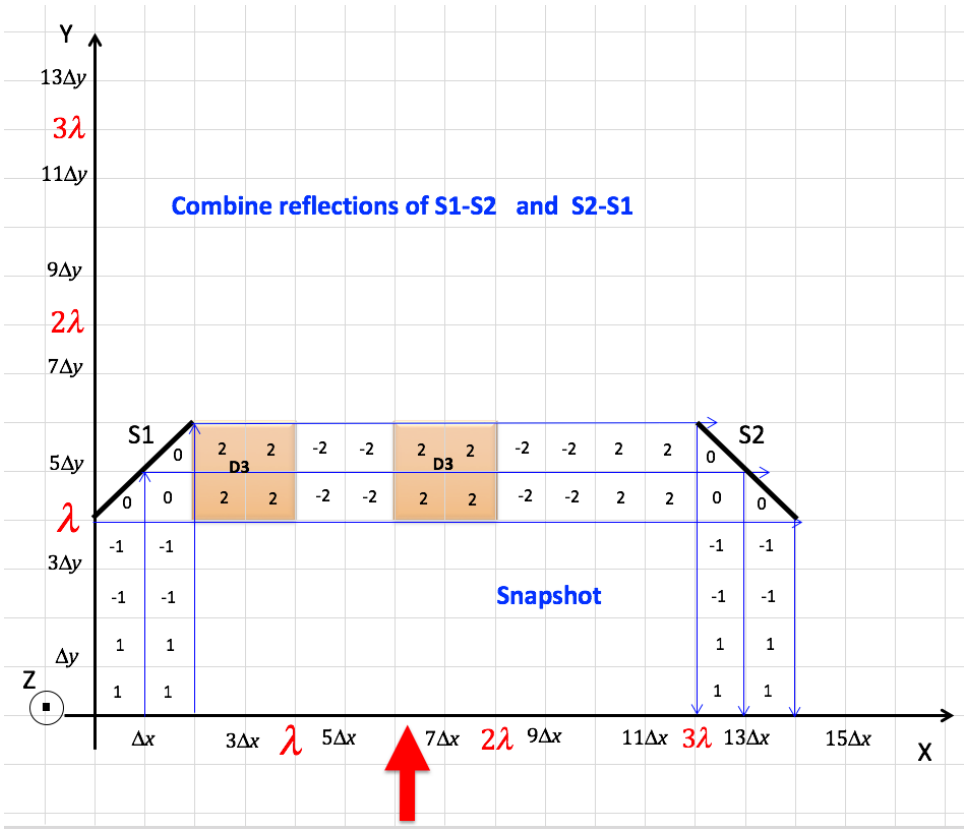

Figure 3.20: Combined fields - incident and all reflections from surfaces $S1$ and $S2$.

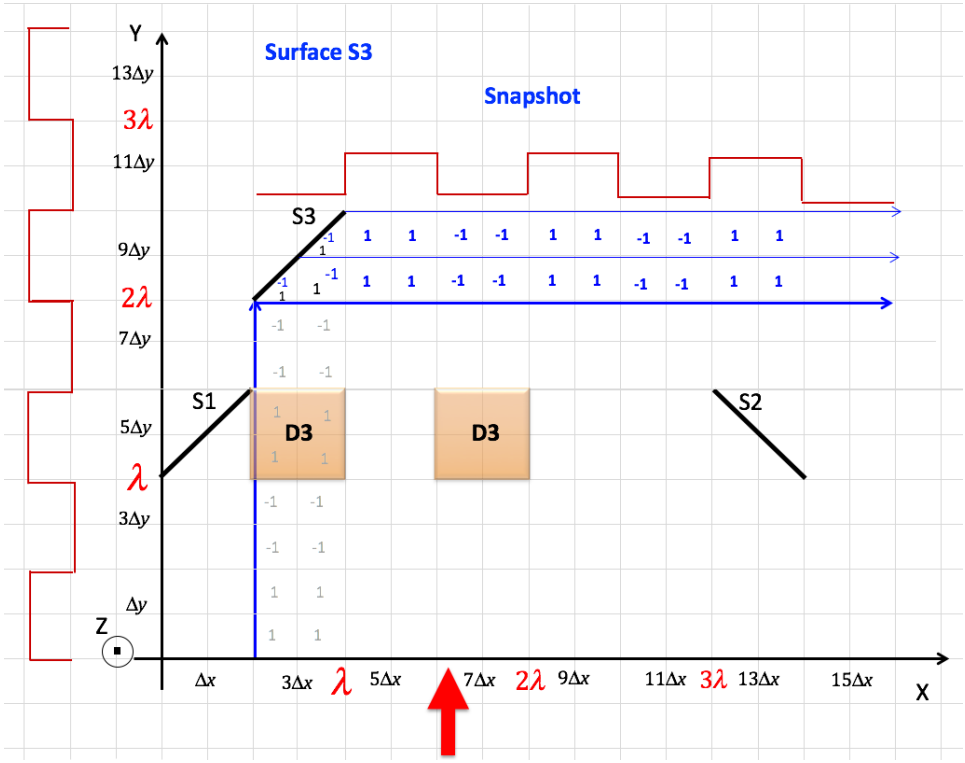

Figure 3.21: Surface $S3$ and surface $S4$ contribute in-phase fields at desired location.

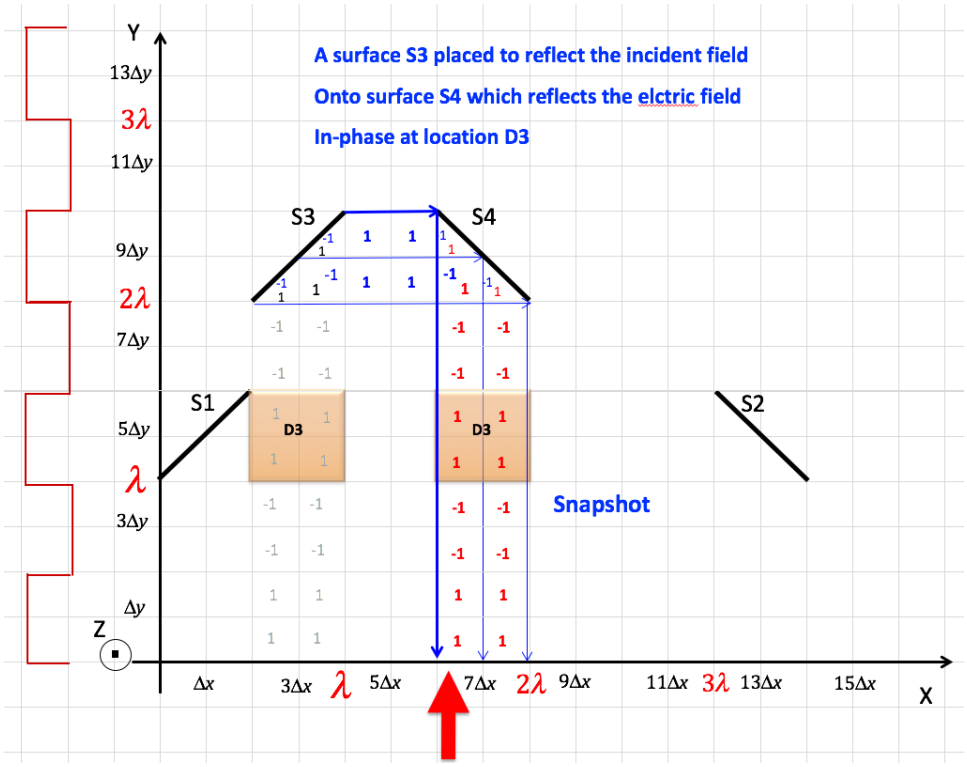

Figure 3.22: Surface $S4$ and reflection from surface $S3$, field in phase at $D3$.

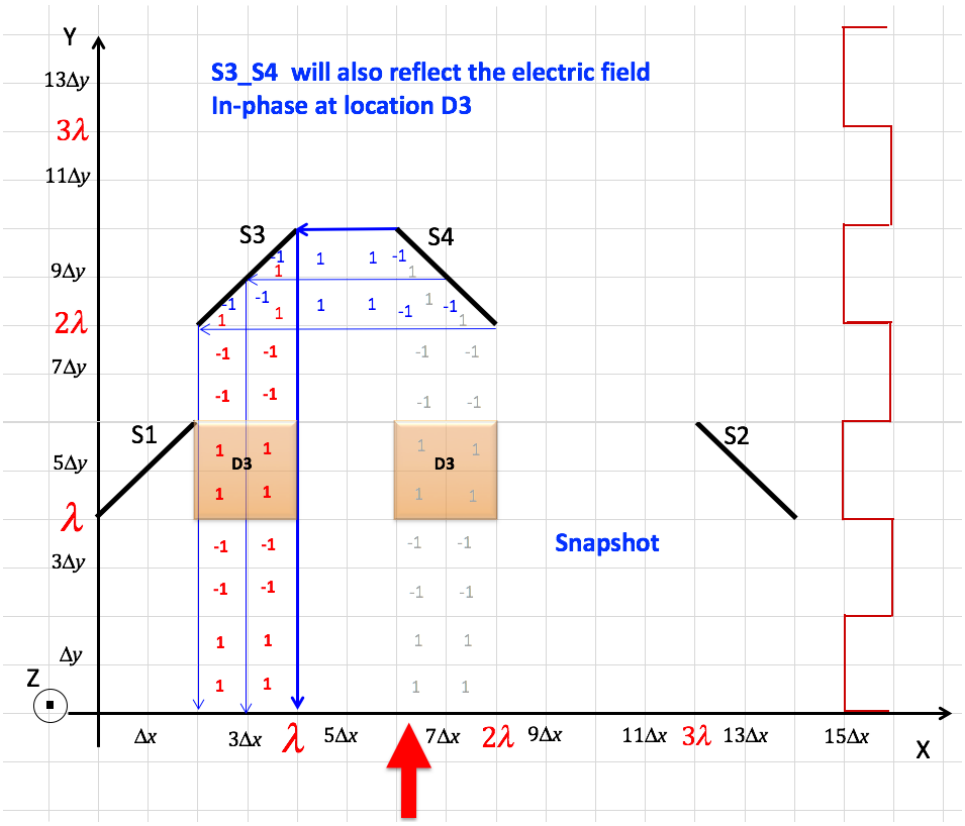

Figure 3.23: Surface $S3$ and reflection from surface $S4$, field in phase at $D3$.

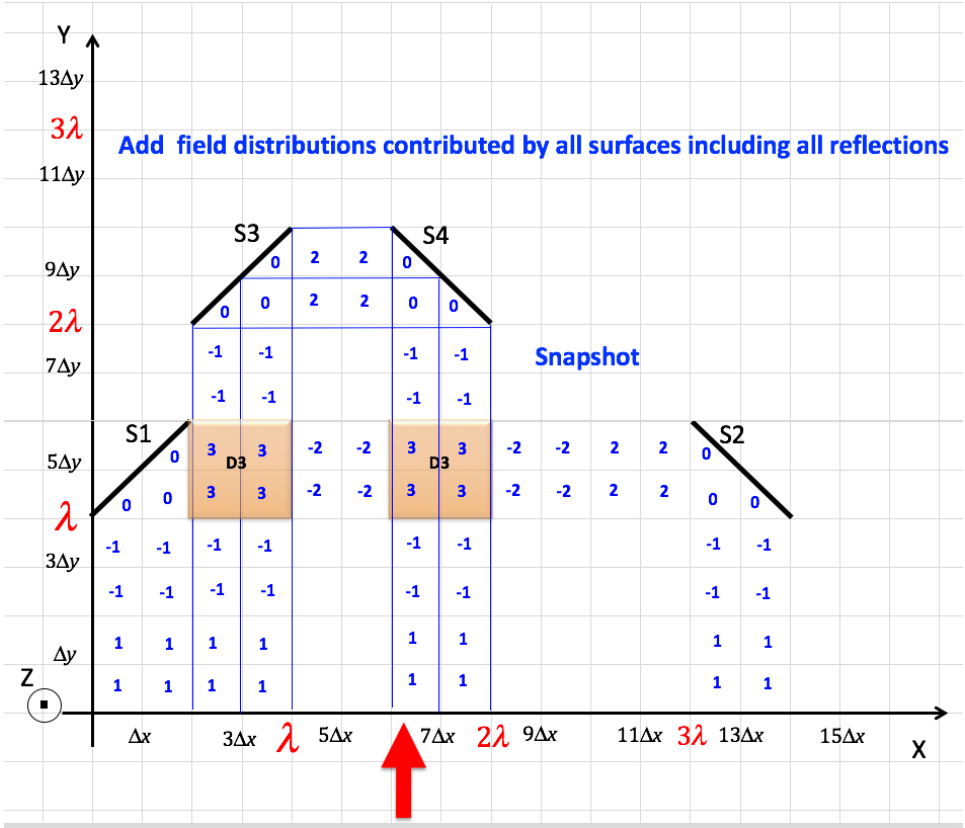

Figure 3.24: All surface reflection, field in phase at $D3$.

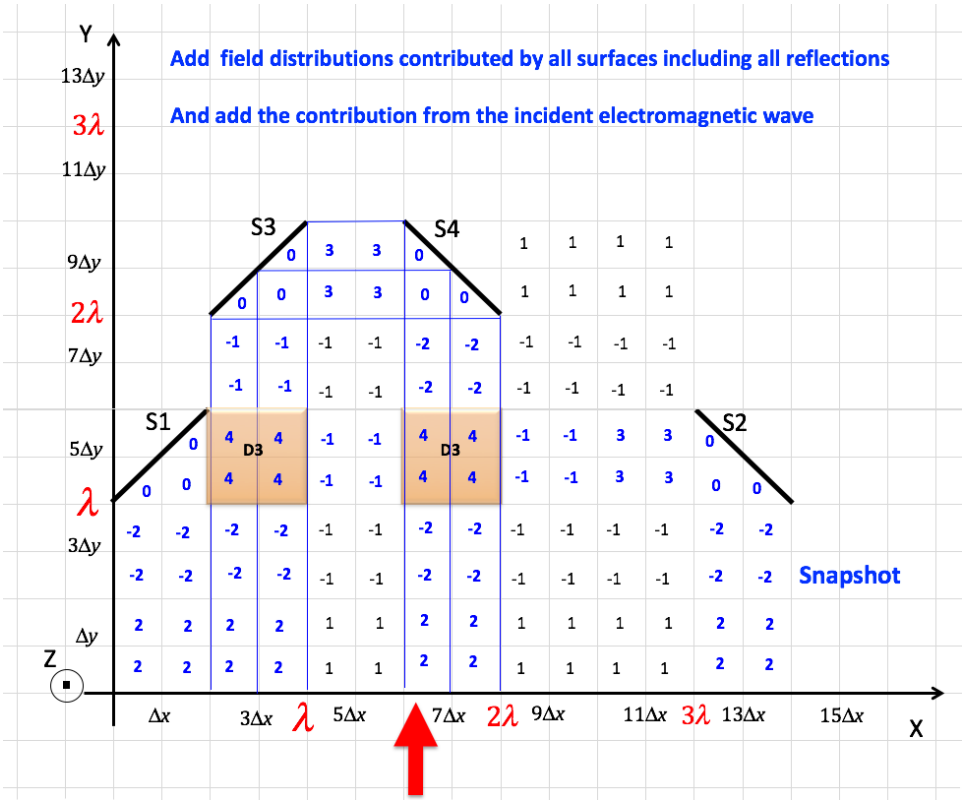

Figure 3.25: Geometric features for providing desired field distribution.

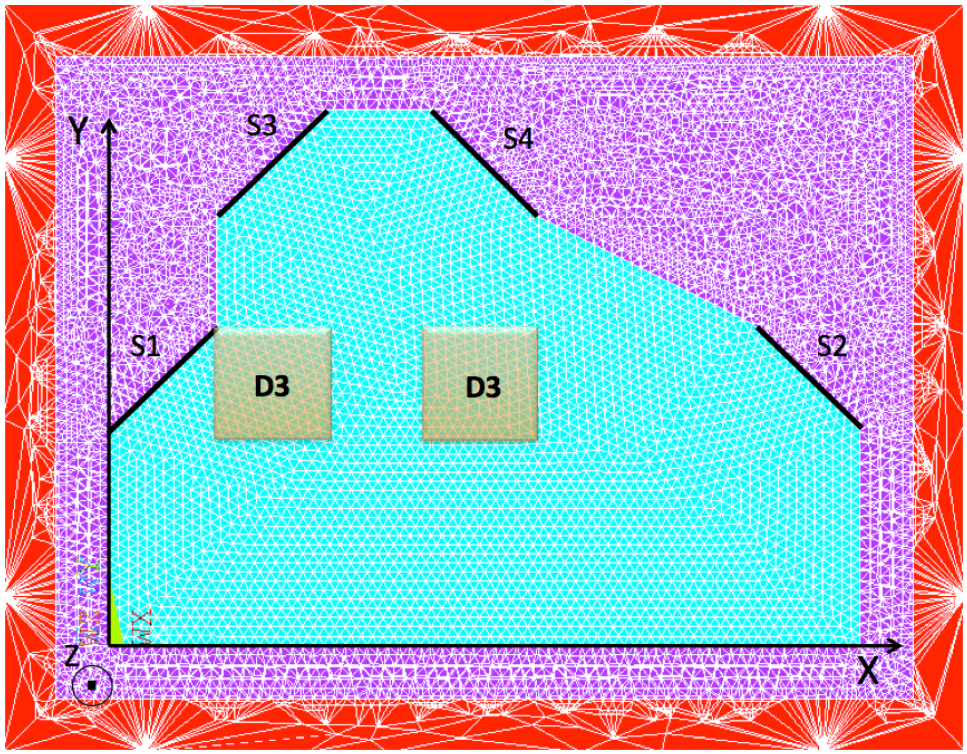

Figure 3.26: Surfaces and geometries analyzed in ANSYS.

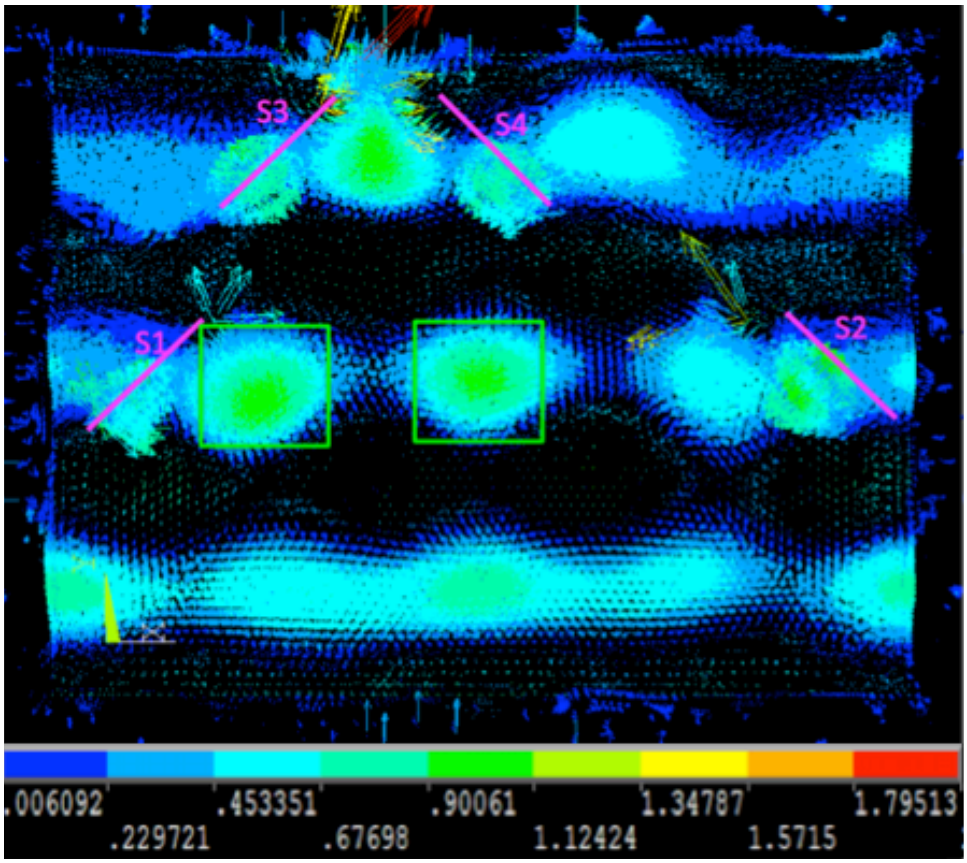

Figure 3.27: Geometry analyzed in ANSYS shows field distributions strongly match with results obtained with developed inverse design method in Figure. 3.26.

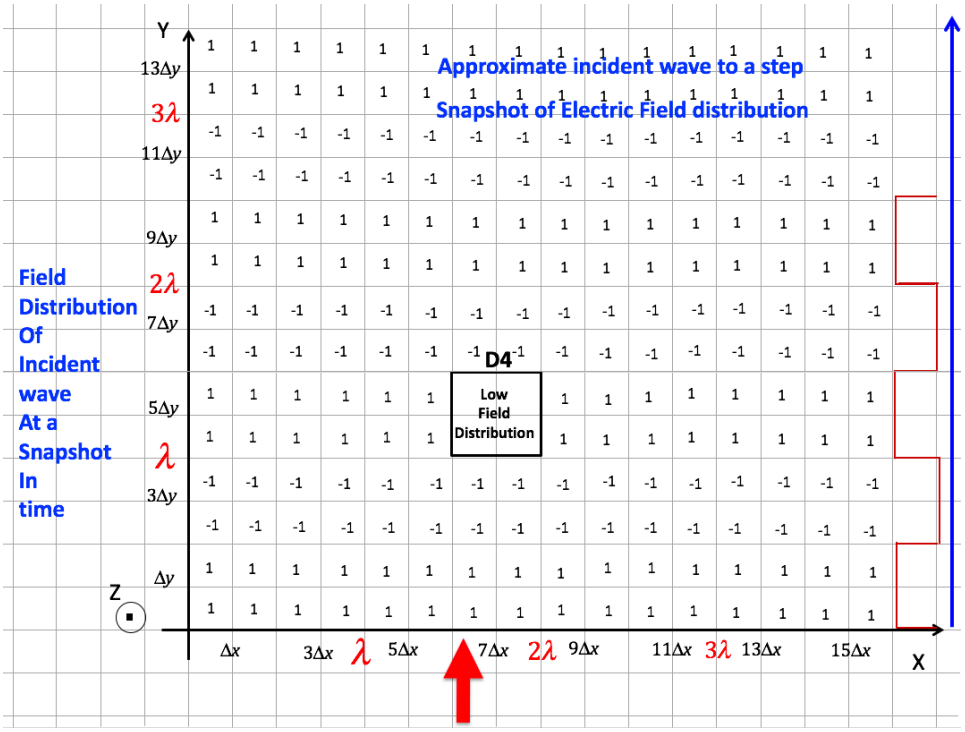

Figure 3.28: Desired low field distribution at location.

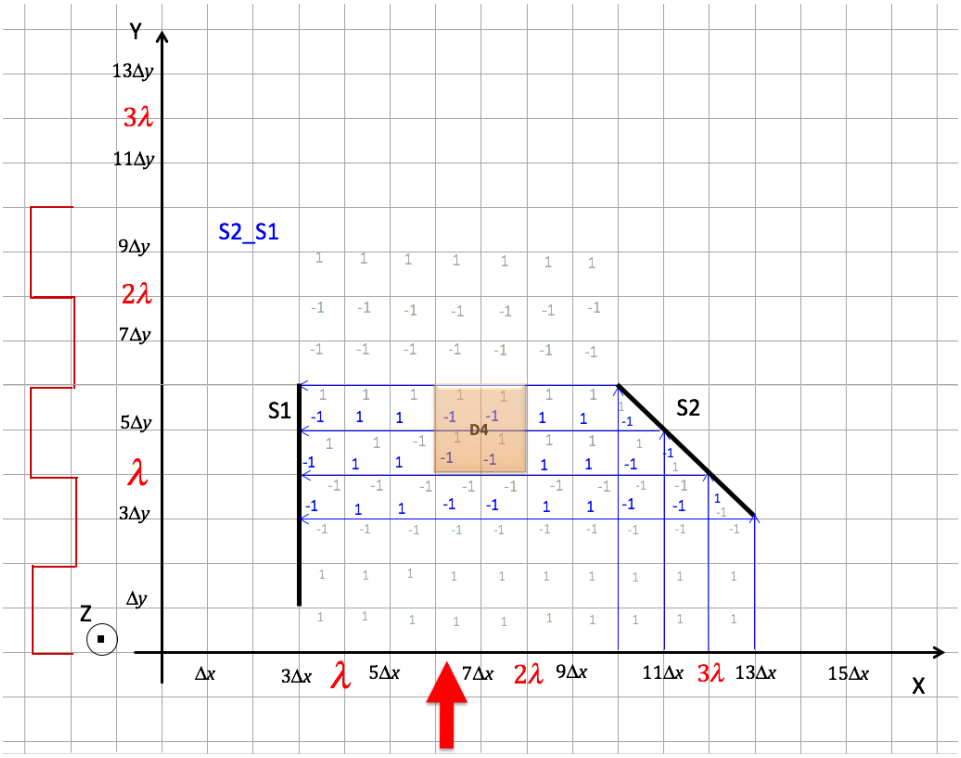

Figure 3.29: Surface $S1$ appropriately placed for reflected fields to be out-of-phase at $D4$.

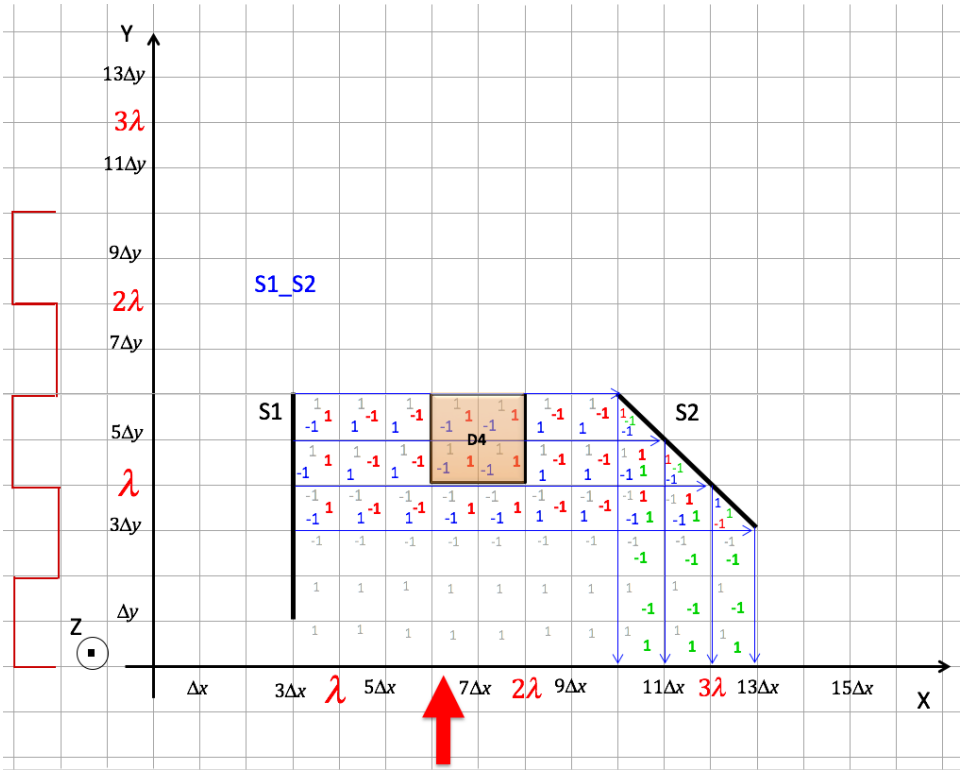

Figure 3.30: Reflection of fields from Surface $S2$ contribute out-of-phase fields at $D4$.

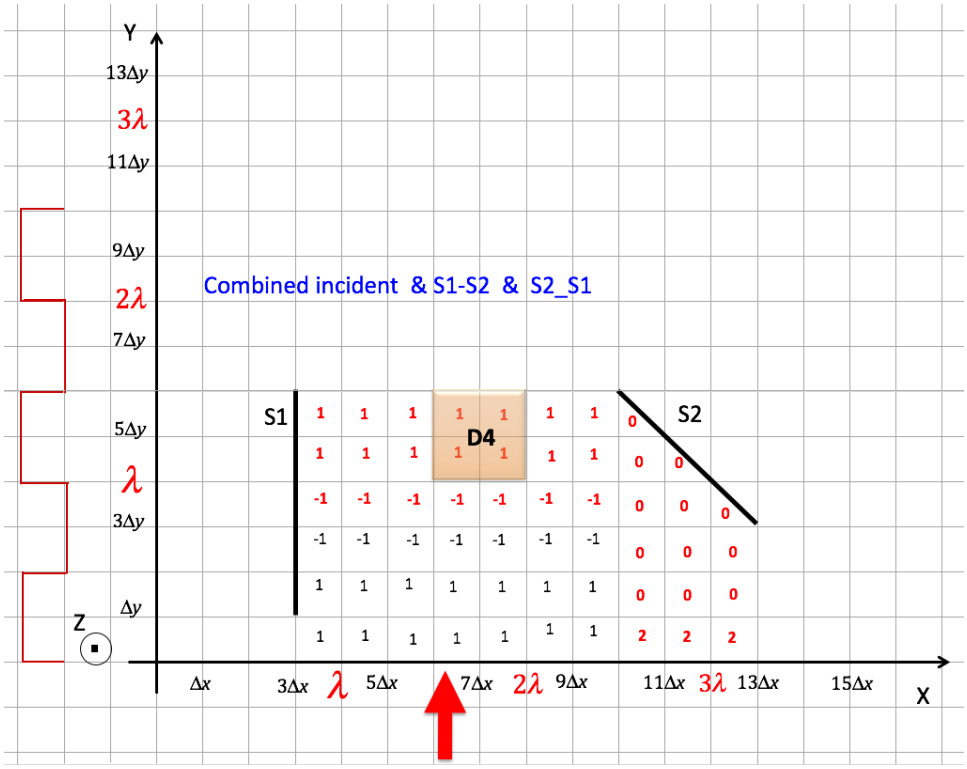

Figure 3.31: Combined fields from incident energy surface $S1$ and surface $S2$.

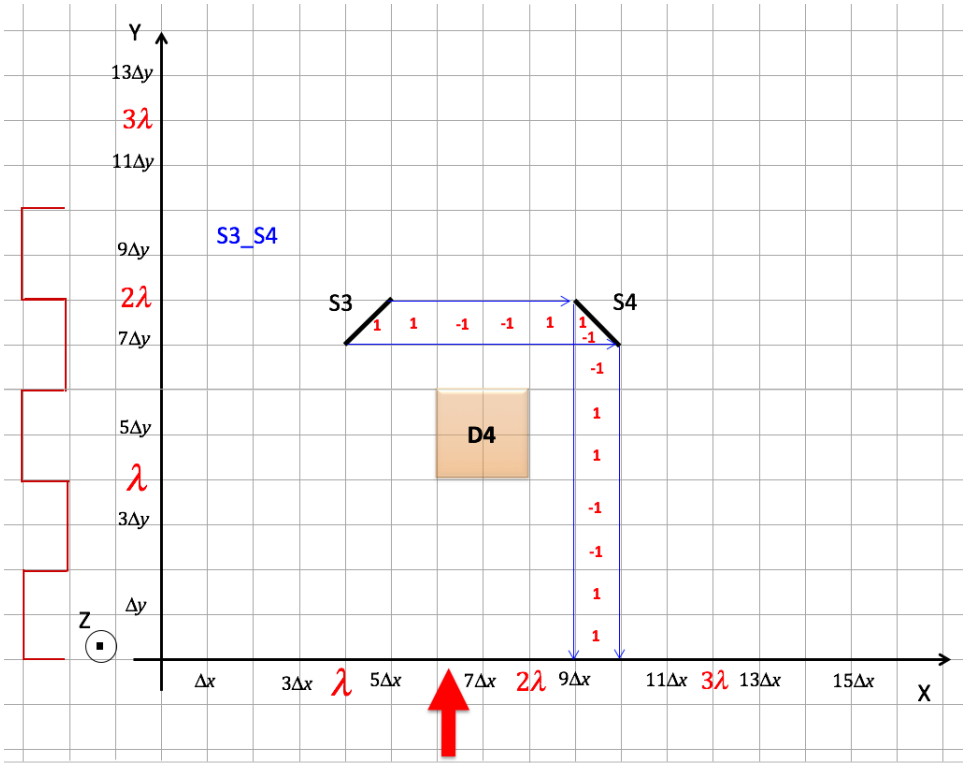

Figure 3.32: Surface $S1$ and $S4$ contribute additional out-of-phase fields.

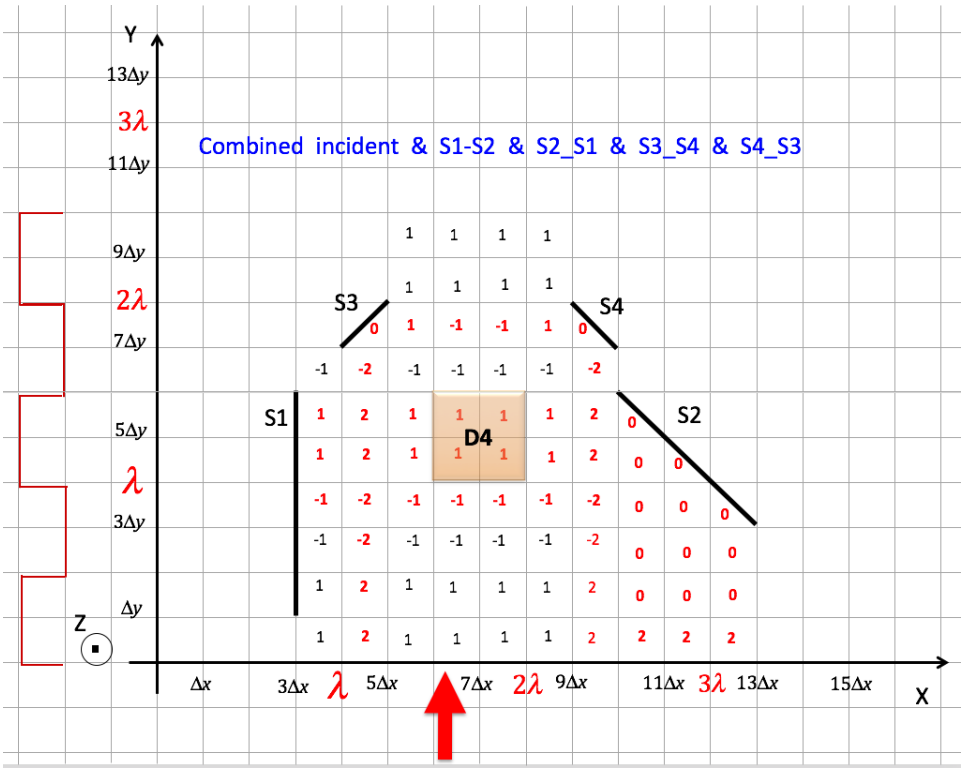

Figure 3.33: Combined field contributions.

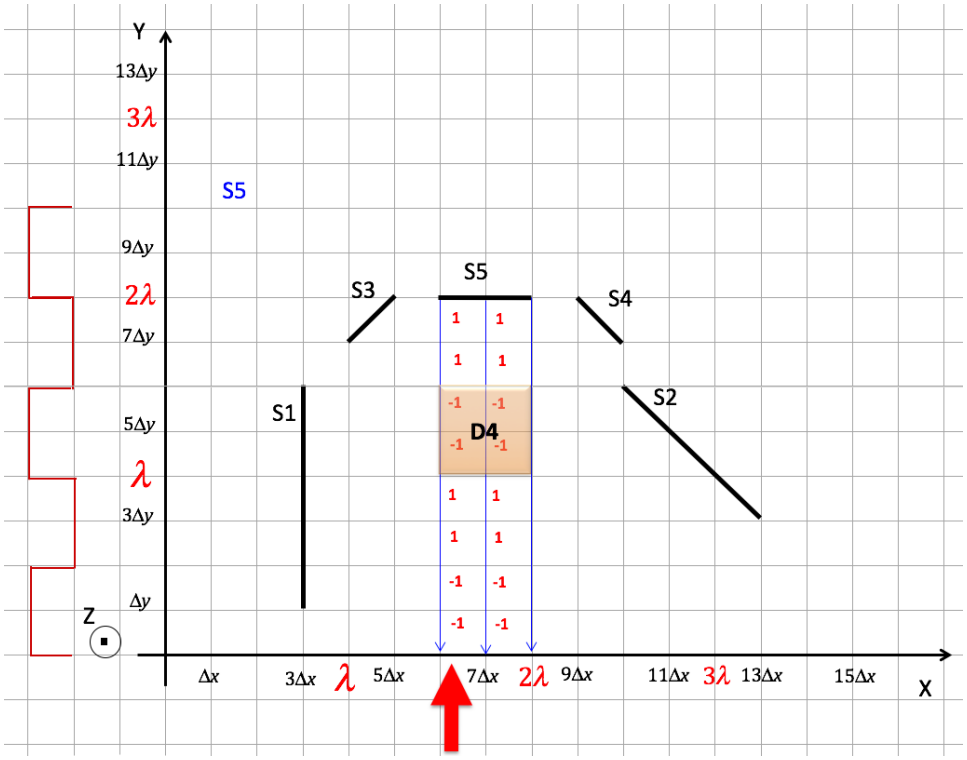

Figure 3.34: Surface $S5$ field contributions at location $D5$.

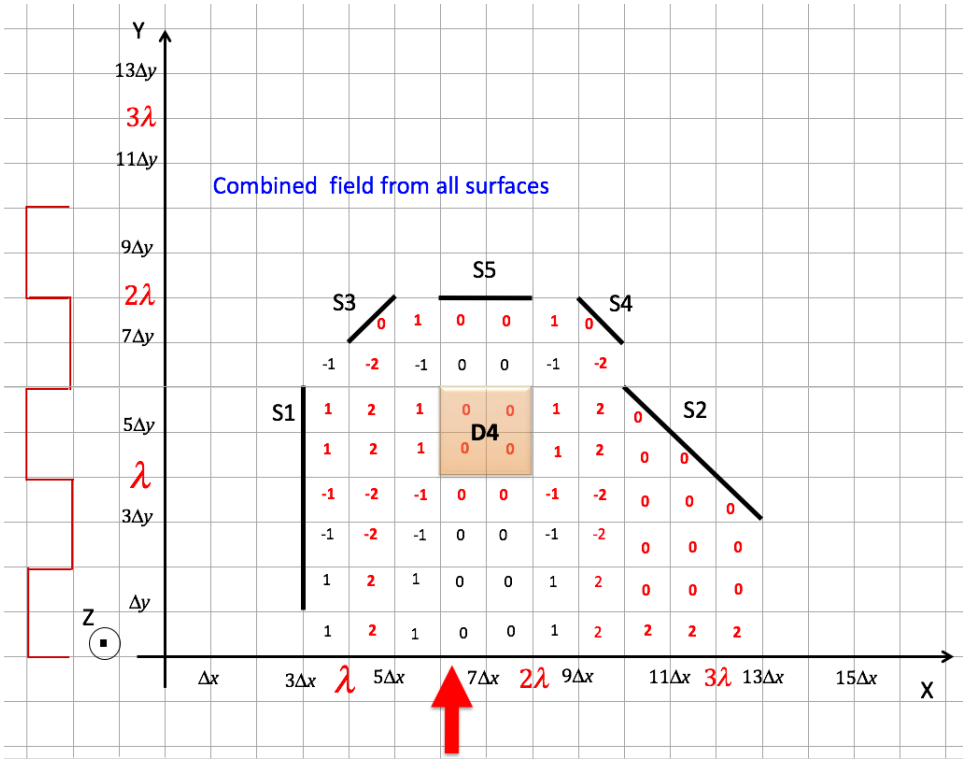

Figure 3.35: All field contributions including all surfaces and Incident fields.

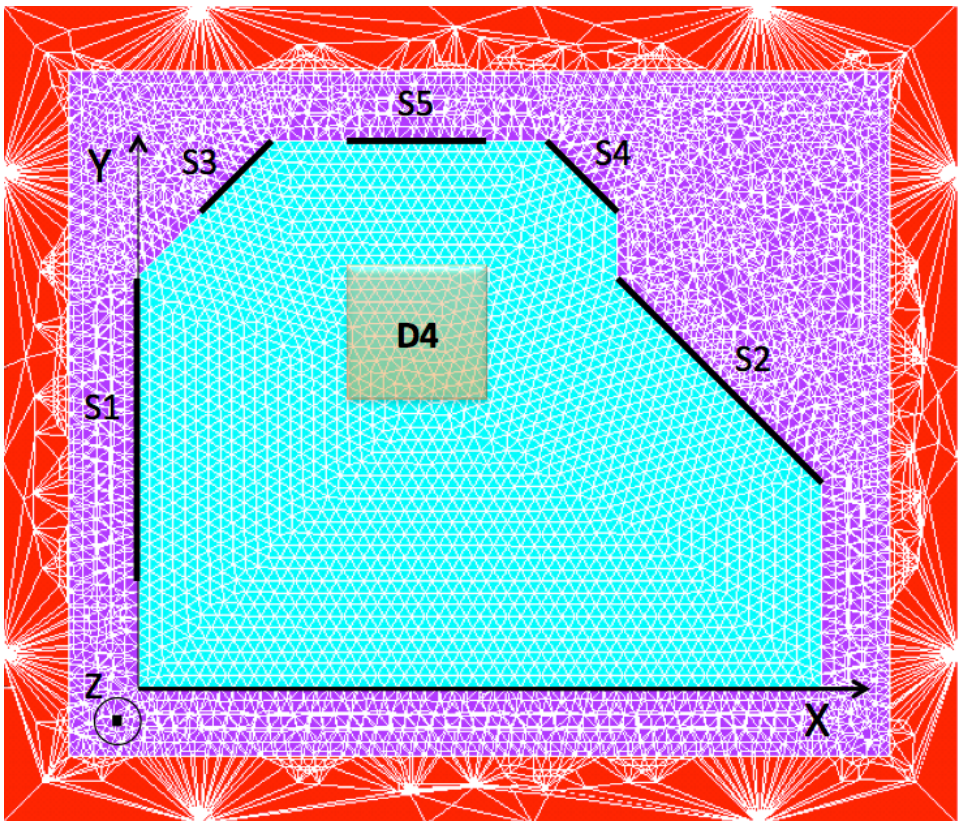

Figure 3.36: ANSYS analysis.

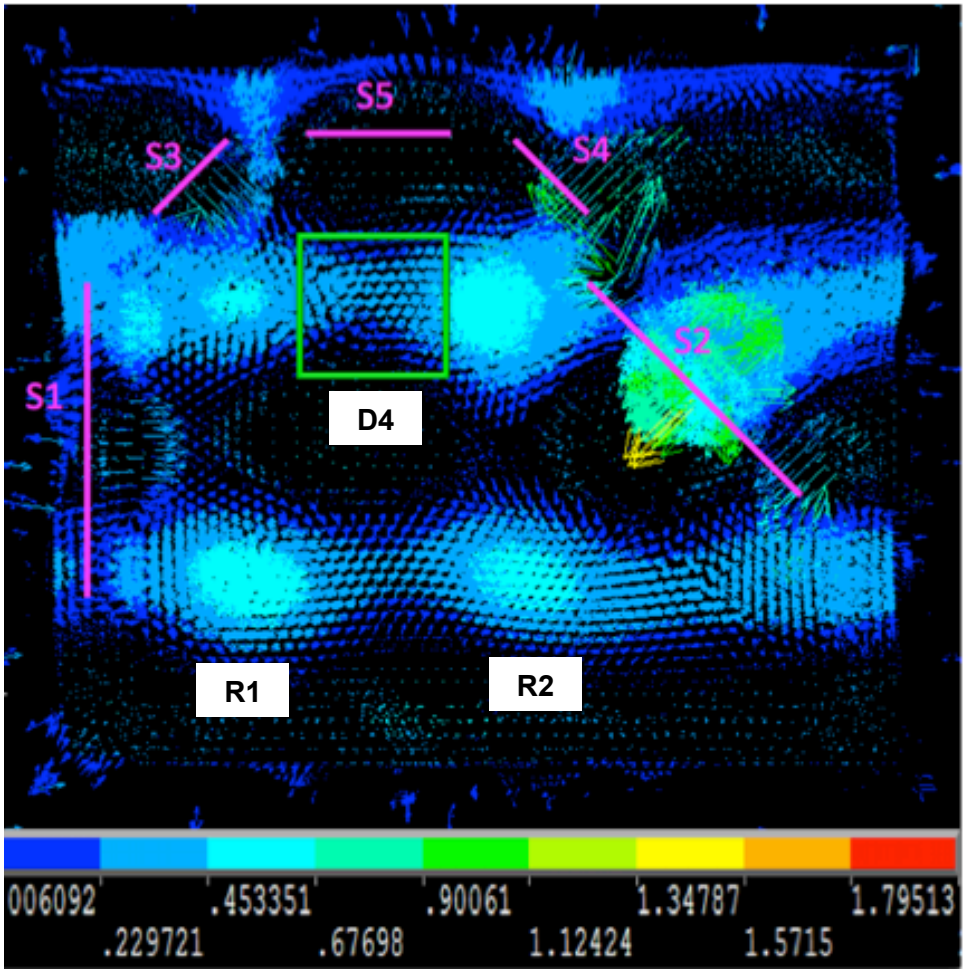

Figure 3.37: ANSYS analysis shows strong correlation with geometry obtained with inverse design method presented.

Chapter 4

Conclusions and future work

The developed method provides a design tool that can easily and rapidly provide geometrical structures that provide a prescribed electrical field distribution for one or more incident electromagnetic waves. The method can also be used for the design of geometrical structures to achieve a prescribed radiation pattern for one or more given electromagnetic radiation sources. As such, the developed method provides not only the analysis tools for determining the distribution of the electric field in a given geometrical structure, but it also provides the tools to perform the inverse of the analysis process, i.e., to design a geometrical structure that would yield a prescribed field distribution for one or more incident waves. The main contribution of the present research work is the development such a simple but powerful method.

The present powerful method can be used to determine steady state as well as transient electric field distribution in any geometrical cavity constructed with arbitrarily shaped surfaces with different material characteristics when interacting with one or more polarized or non-polarized incident waves with

fixed or varying amplitude and/or frequency. The method was shown to work for electromagnetic waves, but is readily seen to work with almost any other wave types with any fixed or varying frequencies. The user must obviously note that spatial discretization must consider the wavelength of the shortest incident wave. The time increments between each field distribution snapshots must also be considered to ensure that they are significantly smaller than half or even a quarter of the wave periods. The obtained field distributions and their time history may be determined with any accuracy by appropriately sizing the grid sizes and the time intervals. The method also can be seen to ready handle the presence of dielectric materials, even with spatially varying physical characteristics.

Designers of radiating or receiving structures now have a new design tool to solve inverse problems involving the design of radiating or receiving geometrical structures to achieve a desired radiation pattern for devices that are designed to efficiently convert timevarying electrical signals into electromagnetic waves, i.e., antennas. In a similar manner, these electrical devices and their geometrical features play a key role when incident electromagnetic waves are to be converted into time-varying electrical signals. The latter devices may be energy harvesting devices, or sensors of some sort, or be devices that are to be designed to minimize the effects of electromagnetic radiation reaching certain of its components.

The four examples presented in chapter 3 clearly show that the design methodology presented in this thesis enables rapid development of sensor structures to achieve the desired spatial distribution of the electric field. The design methodology is easily implemented using low power computational resources to

accommodate more complex structures requiring a large number of interacting surfaces, which have arbitrary shape, orientation and location. Additionally, these arbitrary geometric features can be modeled to include frequency and polarization dependent scattering and reflective properties and can either be distributed or contiguous. A library of such geometric features with known relationship between the incident and reflected (or scattered) electric field can be created to enhance the design process. It is envisioned that any arbitrary spatial distribution of the electric field can be obtained by a combination of these geometric elements located and oriented within the solution space. An algorithm can be developed for coming up with a number of possible inverse solutions from which the user may interactively select and fine tune the sensor design.

Finally, the focus of this work has been on the development of a design tool that can be used to rapidly design complex geometrical structures for a prescribed field distribution. The future work includes its extension to three-dimensional geometries and the development of user friendly software with the capability of allowing the user to undertake the described process in a more predictive manner with the goal of achieving optimal solutions based on the provided design criteria. Indeed, a software tool, comprising of a library of typical geometric shapes and surfaces can be created to visualize the process of design. In other words, imagine a 3-D mapping of the electric field, which changes in real time as one or more of the geometrical features is dragged and oriented in the solution space. This graphical manipulation of the geometric shapes is possible because the computational resources needed for updating the field map are very modest. Such a software tool will enable rapid devel-

opment of new sensor designs across a broad range of frequencies and fields of deployment.

Bibliography

[1] Roger F. Harrington, "Time-harmonic electromagnetic fields", *McGraw-Hill*, 1961, 480pp.

[2] Wang, C., "Advanced computational electromagnetics", *Peking University press*, 2005, ISBN: 730108096.

[3] Ramesh Garg, "Analytical and Computational Methods in Electromagnetics", *Artech House press*, ISBN-13:978-1-59693-385-9

[4] P. Imperatore, A. Iodice, and D. Riccio, "Physical Meaning of Perturbative Solutions for Scattering From and Through Multilayered Structures With Rough Interfaces", *IEEE Trans. Antennas Propag.*, vol. 57, no. 5, pp. 14811494, May 2009.

[5] M. Moghaddam, Y. Rahmat-Samii, E. Rodriguez, D. Entekhabi, J. Hoffman, D. Moller, L. E. Pierce, S. Saatchi, and M. Thomson, "Microwave Observatory of Subcanopy and Subsurface (MOSS): A mission concept for global deep soilmoisture observations", *IEEE Trans. Geosci. Remote Sensing*, vol. 45, no. 8, pp. 26302643, Aug. 2007.

[6] D. J. Daniels, "Ground Penetrating Radar", *Institution of Engineering and Technology*, 2nd ed. London, U.K.: IEE, 2004.

[7] A. G. Yarovoy, R. V. de Jongh, and L. P. Ligthard, "Scattering properties of a statistically rough interface inside a multilayered medium," *Radio Sci.*, vol. 35, no. 2, pp. 455462, 2000.

[8] A. G. Yarovoy, R. V. de Jongh, and L. P. Ligthart, "Transmission of electromagnetic fields through an air-ground interface in the presence ofstatistical roughness," *in Proc. IEEE IGARSS98, Seattle, WA*, Jul. 610, 1998, vol. 3, pp. 14631465.

[9] R. Azadegan and K. Sarabandi, "Analytical formulation of the scattering by a slightly rough dielectric boundary covered with a homogeneousdielectriclayer," *in Proc. IEEE AP-S Int. Symp., Columbus, OH,* Jun. 2003, pp.420423.

[10] A. Fuks, "Wave diffraction by a rough boundary of an arbitrary plane layered medium," *IEEE Trans. Antennas Propag.*, vol. 24, pp. 630639, 2001.

[11] G. Franceschetti, P. Imperatore, A. Iodice, D. Riccio, and G. Ruello, "Scattering from layered medium with one rough interface: Comparison and physical interpretation of different methods," *in Proc. IEEE IGARSS, Toulouse, France*, Jul. 2003, pp. 29122914.

[12] G. Franceschetti, P. Imperatore, A. Iodice, D. Riccio, and G. Ruello, "Scattering from layered structures with one rough interface: A unified formulation of perturbative solutions," *IEEE Trans. Geosci. Remote Sens.*, vol. 46, no. 6, Jun. 2008.

[13] I. M. Fuks, "Radar contrast polarization dependence on subsurface sensing," *in Proc. IEEE IGARSS98, Seattle,WA*, Jul. 610, 1998, vol. 3, pp. 14551459.

[14] A. Kalmykov, I. Fuks, I. Scherebinin, V. Tsymbal, A. Matveev, A. Gavrilekno, M. Fix, and V. Freilikher, "Radar observations of strong subsurface scatterers. A model of backscattering," *in Proc. IEEE IGARSS95*, 1995, vol. 3, pp. 17021704.

[15] I. M. Fuks and A. G. Voronovich, "Interference phenomena in scattering by rough interfaces in arbitrary plane-layered media," *in Proc. IGARSS*, 2000, vol. 4, pp. 17391741.

[16] A. Tabatabaeenejad and M. Moghaddam, "Bistatic scattering from three-dimensional layered rough surfaces," *IEEE Trans. Geosci. Remote Sensing*, vol. 44, no. 8, pp. 2102 2114, Aug. 2006.

[17] P. Imperatore, A. Iodice, and D. Riccio, "Electromagnetic wave scattering from layered structures with an arbitrary number of rough interfaces," *IEEE Trans. Geosci. Remote Sensing*, vol. 47, no. 4, pp. 10561072, April 2009.

[18] P. Imperatore, A. Iodice, and D. Riccio, "Transmission through layered media with rough boundaries: First-order perturbative solution," *IEEE Trans. Antennas Propag.*, vol. 57, no. 5, pp. 14811494, May 2009.

[19] Michael J. Bluck, A. Hatzipetros, S. P. Walker, "Applications of Differential Forms to Boundary Integral Equations", *IEEE TRANSACTIONS ON ANTENNAS AND PROPAGATION*, VOL. 54, NO. 6, JUNE 2006

[20] R. Hiptmair, "Finite elements in computational electromagnetism," *Acta. Numerica.*, vol. 11, p. 237, 2002.

[21] "Canonical construction of finite elements," *Math. Comput.*, vol. 68, p. 1325, 1999.

[22] P. W. Gross and P. R.Kotiuga, "Data structures for geometric and topological aspects of finite element algorithms," *J. Electromagn. Waves Applicat.*, vol. 15, p. 257, 2001.

[23] A. Bossavit, "Generating Whitney forms of polynomial degree one and higher," *IEEE Trans. Magn.*, vol. 38, p. 341, 2002.

[24] "Mixed systems of algebraic equations in computational electromagnetism," *COMPELThe Int. J. Comput. Math. Elect. Electron. Eng.*, vol. 17, no. 1, p. 59, 1998.

[25] "Differential forms and the computation of fields and forces in electromagnetism," *Eur. J. Mechan.*, B/Fluids, vol. 10, p. 474, 1991.

[26] S. M. Rao, D. R. Wilton, and A. W. Glisson, "Electromagnetic scattering by surfaces of arbitrary shape," *IEEE Trans. Antennas Propag.*, vol. AP-30, p. 409, 1982.

[27] Krzysztof A, Michalski, Dalian Zheng, "Electromagnetic Scatteringand Radiation by Surfaces of Arbitrary Shape in Layered Media, Part I: Theory", *IEEE TRANSACTIONS ON ANTENNAS AND PROPAGATION*, VOL. 38. NO. 3. MARCH 1990

[28] Sadasiva M. Rao. Donald R. Wilton, "Electromagnetic Scattering by Surfaces of Arbitrary Shape" , *IEEE TRANSACTIONS ON ANTENNAS AND PROPAGATION*, VOL. AP-30, NO. 3, MAY 1982

[29] W. Cai, T. Yu, H. Wang, and Y. Yu, "High-order mixed RWG basis functions for electromagnetic applications," *IEEE Trans. Microw. Theory Tech.*, vol. 49, no. 7, p. 1295, Jul. 2001.

[30] C. J. Huber, W. Rieger, M. Haas, and W. M. Rucker, "Application of curvilinear higher order edge elements to scattering problems using the boundary element method," *IEEE Trans. Magn.*, vol. 35, no. 3, p. 1510,May 1999.

[31] J. C. Nedelec, "Mixed finite elements in ," *Numerische Mathematik*, vol. 35, p. 315, 1980.

[32] R. Hiptmair, "Higher order Whitney forms," *J. Electromagn. Waves Applicat.*, vol. 15, p. 341, 2001.

[33] "Higher order whitney forms," *in Geometrical Methods for Computational Electromagnetics* (in Progress in Electromagnetic Research, F. L. Teixeira, Ed. Cambridge, U.K.:EMWPublishing, 2001, vol. 32, pp. 271299.

[34] K. F. Warnick, D. V. Arnold, and R. H. Selfridge, "Differential Forms in Electromagnetic Field Theory," *in Proc. IEEE Antennas Propagation Symp.*, Baltimore, MD, Jun. 1996, pp. 14741477.

[35] S. Kurz, O. Rain, V. Rischmuller, and S. Rjasanow, "Discretization of boundary integral equations by differential forms on dual grids," *IEEE Trans. Magn.*, vol. 40, p. 826, 2004.

[36] Charles J. Daly, Todd W. Nuteson "The Spatially Averaged Electric Field in the Near Field and Far Field of a Circular Aperture", *IEEE TRANSACTIONS ON ANTENNAS AND PROPAGATION*, VOL. 51, NO. 4, APRIL 2003

[37] C. Bouwkamp, "Theoretical and numerical treatment of diffraction through a circular aperture," *IEEE Trans. Antennas Propagat.*, vol. AP-18, pp. 152176, Mar. 1970.

[38] F. Northover, "Applied Diffraction Theory". *New York: American Elsevier*,1971.

[39] E. Lommel, "Die beugungserserscheinungen ether kreisrunden ffnungund eines kreisrundes schirmes (Diffraction by a circular aperture or a circular disk)," *Abh. der math. phys. Classe der k. b. Akad. der Wiss.*, vol. XV, pp. 229328, 1886.

[40] J. Sherman III, "Aperture-antenna analysis," in Radar Handbook, M. Skolnik, Ed. Lexington, MA *McGraw-Hill*, 1970, ch. 9.

[41] Le-Wei Li, Pang-Shyan Kooi, Tat-Soon Yeo, "Exact Solutions of Electromagnetic Fields in Both Near and Far Zones Radiated by Thin Circular-Loop Antennas: A General Representation", *IEEE TRANSACTIONS ON ANTENNAS AND PROPAGATION,* VOL. 45, NO. 12, DECEMBER 1997

[42] D. H. Werner, "An exact integration procedure for vector potentials of thin circular loop antennas," *IEEE Trans. Antennas Propagat.*, vol. 44, pp. 157165, Feb. 1996.

[43] P. L. Overfelt, "Near fields of the constant current thin circular loop antenna of arbitrary radius," *IEEE Trans. Antennas Propagat.*, vol. 44, pp. 166171, Feb. 1996.

[44] D. Foster, "Loop antennas with uniform current," *Proc. IRE*, vol. 32, pp. 603607, Oct. 1944.

[45] J. B. Sherman, "Circular loop antennas with uniform current," *Proc. IRE*, vol. 32, pp. 534537, Sept. 1944.

[46] G. Glinski, "Note on the circular loop antennas with nonuniform current distribution," *J. Appl. Phys.*, vol. 18, pp. 638644, July 1947.

[47] J. E. Lindsay, Jr., "A circular loop antenna with nonuniform current distribution," *IRE Trans. Antennas Propagat.*, vol. AP-8, pp. 439441, July 1960.

[48] E. J. Martin, Jr., "Radiation fields of circular loop antennas by a direct integration process," *IRE Trans. Antennas Propagat.*, vol. AP-8, pp.105107, Jan. 1960.

[49] T. T. Wu, "Theory of the thin circular loop antenna," *J. Math. Phys.,* vol. 3, pp. 13011304, 1962.

[50] F. M. Greene, "The near-zone magnetic field of a small circular-loop antenna," *J. Res. NSB*, vol. 71-C, no. 4, pp. 319326, Oct. 1967.

[51] B. R. Rao, "Far-field patterns of large circular loop antennas: Theoretical and experimental results," *IEEE Trans. Antennas Propagat.*, vol. AP-16, pp. 269270, Mar. 1968.

[52] S. M. Prasad and B. N. Das, "A circular loop antenna with traveling wave current distribution," *IEEE Trans. Antennas Propagat.*, vol. AP-18, pp. 278280, Mar. 1970.

[53] G. S. Smith, "Loop antennas," in Antenna Engineering Handbook. *New York: McGraw-Hill*, 1984.

[54] P. L. Overfelt, "Near Fields of the Constant Current Thin Circular Loop Antenna of Arbitrary Radius", *IEEE TRANSACTIONS ON ANTENNAS AND PROPAGATION*, VOL. 44, NO. 2, FEBRUARY 1996

[55] C. A Balanis, "Antenna Theory, Analysis, and Design". *New York*

[56] S. A. Schehnoff, " AdvancedAntennu Theory". *New York: Wiley*, 1952.

[57] "R. S. Elliott, Antenna Theory and Desian. Englewood Cliffs." *NJ: Wiley*, 1982, ch. 5. . Prentice-Hall, 1981.

[58] J. D. Kraus, "Antennas". *New York McGraw-Hill*, 1950.

[59] R. E. Collin and F. J. Zucker, "Antenna Theory, Part I". *New York: McGraw-Hill*, 1969, ch. 11.

[60] W. L. Stutzman and G. A. Thiele, "Antenna Theory and Desian". *New York: Wiley*, 1981, ch. 2.

[61] W. L. Weeks, "Electromagnetic Theory for Engineering Applications". *New York Wiley*, 1964, ch. 7.

[62] S. A. Adekola, "On the excitation of a circular loop antenna by travelling- and standing-wave current distributions," *Int. J. Electron.*, vol. 54, p. 705, 1983.

[63] W. R. Smythe, "Static and Dynamic Electricity". *New York: McGraw-Hill*, 1950, pp. 488490.

[64] F. M. Greene, "The near-zone magnetic field of a small circular loop antenna," *J. Res. Nut. Bur. Stds.-C*, vol. 71-C, pp. 319-326, 1967.

[65] T. T. Wu, "Theory of the thin circular loop antenna," *J. Math. Phys.*, vol. 3, pp. 1301-1304, 1962.

[66] P. L. Overfelt, "An exact method of integration for vector potentials of thin dipole antennas," *IEEE Trans. Antennas Propagat.*, vol. AP-35, pp. 442-444, 1987.

[67] A. E. Ciera, "Comments on An exact method of integration for vector potentials of thin dipole antennas (and authors reply)," *IEEE Trans. Antennas Propagat.*, vol. 38, p. 584, 1989.

[68] D. H. Werner, "An exact formulation for the vector potential of a cylindrical antenna with uniformly distributed current and arbitrary radius," *IEEE Trans. Antennas Propagat.*, vol. 41, p. 1009, 1993.

[69] RongLin Li; Bushyager, N.A.; Laskar, J.; Tentzeris, M.M. "Determination of reactance loading for circularly polarized circular loop antennas with a uniform traveling-wave current distribution", *Antennas and Propagation, IEEE Transactions on*, pp. 3920 - 3929 Volume: 53, Issue: 12, Dec. 2005 Abstract — Full Text: PDF (1160KB).

[70] Werner, D.H.; Werner, P.L. "Near-zone expansions for the vector potential of the traveling-wave current loop antenna", *Antennas and Propagation Society International Symposium*, 1996. AP-S. Digest, On page(s): 844 - 847 vol.2 Volume: 2, 21-26 July 1996

[71] Le-Wei Li; Mui-Seng Yeo; Mook-Seng Leong "Method of moments analysis of EM fields in a multilayered spheroid radiated by a thin circular loop antenna", *Antennas and Propagation, IEEE Transactions on*, pp: 2391 - 2402 Volume: 52, Issue: 9, Sept. 2004

[72] Werner, D.H. "An exact integration procedure for vector potentials of thin circular loop antennas", *Antennas and Propagation, IEEE Transactions on*, pp: 157 - 165 Volume: 44, Issue: 2, Feb 1996

[73] Le-Wei Li; Mook-Seng Leong; Pang-Shyan Kooi; Tat-Soon Yeo "Exact solutions of electromagnetic fields in both near and far zones radiated by thin circular-loop antennas: a general representation ", *Antennas and Propagation, IEEE Transactions on*, pp: 1741 - 1748 Volume: 45, Issue: 12, Dec 1997

[74] Franceschetti, G.; Papas, Charles H. "Pulsed antennas", *Antennas and Propagation, IEEE Transactions on*,pp: 651 - 661 Volume: 22, Issue: 5, Sep 1974

[75] Langenberg, K. "Transient fields of small loop antennas", *Antennas and Propagation, IEEE Transactions on*, pp: 236 - 239 Volume: 24, Issue: 2, Mar 1976

[76] F. Seydou, Tapio Seppnen, Omar M. Ramahi, "Computation of the Helmholtz Eigenvalues in a Class of Chaotic Cavities Using the Multipole" *Expansion Technique*

[77] M. C. Gutzwiller, "Chaos in Classical and Quantum Mechanics". *New York: Springer*, 1990.

[78] V. Galdi, I. M. Pinto, and L. B. Felsen, "Wave propagation in raychaotic enclosures: Paradigms, oddities and examples," *IEEE Antennas Propag. Mag.*, vol. 47, pp. 6281, Feb. 2005.

[79] S. Hemmady, X. Zheng, E. Ott, T. Antonsen, and S. Anlage, "Universalimpedance fluctuations in wave chaotic systems," *Phys. Rev. Lett.*, vol. 94, p.014102, 2005.

[80] S. Hemmady, X. Zheng, T. Antonsen, E. Ott, and S. Anlage, "Universal statistics of the scattering coefficient of chaotic microwave cavities," *Phys. Rev. E*, vol. 71, p. 056215, 2005.

[81] M. Hentschel and K. Richter, "Quantum chaos in optical systems: Theannular billiard," *Phys. Rev. E*, vol. 66, p. 056207, 2002

[82] Fikret Altunkilic, Taha S. Imeci, Joseph R. Mautz, "Transmission Through an Arbitrary Aperture in a 3-D Conducting Surface Enclosing Chiral Material"

[83] D. Worasawate, J. R. Mautz, and E. Arvas, "Electromagnetic scattering from an arbitrarily shaped three-dimensional homogeneous chiral body," *IEEE Trans. Antennas Propag.*, vol. 51, no. 5, pp.1077-1084, May 2003.

[84] V. Demir, A. Z. Elsherbeni, and E. Arvas, "FDTD formulation for dispersive chiral media using the Z transform method," *IEEE Trans. Antennas Propag.*, vol. 53, no. 10, pp. 33743384, Oct. 2005.

[85] F. Bilotti, A. Toscano, and L. Vegni, "FEM-BEM formulation for the analysis of cavity-backed patch antennas on chiral substrates," *IEEE Trans. Antennas Propag.*, vol. 51, no. 2, pp. 306311, Feb. 2003.

[86] F. Bilotti, A. Toscano, and L. Vegni, "FEM-BEM formulation for the analysis of cavity-backed patch antennas on chiral substrates," *IEEE Trans. Antennas Propag.*, vol. 51, no. 2, pp. 306311, Feb. 2003.

[87] C. Cristopoulos, J. Paul, and D. W. P. Thomas, "Simulation of EM wave propagation inmagnetoelectric media using TLM," *Int. J. Numer. Model.*, vol. 14, pp. 493505, 2001.

[88] Juhua Liu and Yunliang Long, "A Full-Wave Numerical Approach for Analyzing Rectangular Waveguides With Periodic Slots", *IEEE TRANSACTIONS ON ANTENNAS AND PROPAGATION*, VOL. 60, NO. 8, AUGUST 2012

[89] L. O. Goldstone and A. A. Oliner, "Leaky-wave antennas I: Rectangular waveguides," *IRE Trans. Antennas Propag.*, vol. AP-7, no. 4, pp. 307319, Oct. 1959.

[90] A. A. Oliner and D. R. Jackson, "Leaky-wave antennas," *Antenna Engineering Handbook*, J. L. Volakis, Ed., 4th ed. New York: Mc- Graw-Hill, 2007, ch. 11.

[91] P. J. B. Clarricoats, P. E. Green, and A. A. Oliner, "Slot-mode propagation in rectangular waveguide," *Electron. Lett.*, vol. 2, no. 8, pp. 307308, Aug. 1966.

[92] A. Sutinjo, M. Okoniewski, and R. H. Johnston, "Suppression of the slot-mode radiation in a slotted waveguide using periodic slot perturbation," *IEEE Antennas Wireless Propag. Lett.*, vol. 8, pp. 550553, 2009.

[93] R. S. Elliott, "On the design of traveling-wave-fed longitudinal shunt slot arrays," *IEEE Trans. Antennas Propag.*, vol. 7, no. 5, pp. 717720, Sep. 1979.

[94] W. J. Getsinger, "Elliptically polarized leaky-wave array," *IRE Trans. Antennas Propag.*, vol. 10, no. 2, pp. 165171, Mar. 1962.

[95] R. F. Hyneman, "Closely-spaced transverse slots in rectangular waveguide," *IRE Trans. Antennas Propag.*, vol. 7, pp. 335342, Oct. 1959.

[96] J. Liu, D. R. Jackson, and Y. Long, "Modal analysis of dielectric-filled rectangular waveguide with transverse slots," *IEEE Trans. Antennas Propag.*, vol. 59, no. 9, pp. 31943203, Sep. 2011.

[97] F. L. Whetten and C. A. Balanis, "Meandering long slot leaky-wave waveguide antennas," *IEEE Trans. Antennas Propag.*, vol. 39, no. 11, pp. 15531560, Nov. 1991.

[98] F. L. Whetten and C. A. Balanis, "Effects of a dielectric coating on leaky-wave long-slot waveguide antennas," *IEEE Tran. Antennas Propag.*, vol. 44, no. 8, pp. 11661171, Aug. 1996.

[99] J. Joubert and J. A. G. Malherbe, "Moment method calculation of the propagation constant for leaky-wave modes in slotted rectangular waveguide," *IEE Proc.-Microw. Antennas Propag.*, Dec. 1999, vol. 146, no. 6.

[100] F. Xu, K. Wu, and X. Zhang, "Periodic leaky-wave antenna for millimeter wave applications based on substrate integrated waveguide," *IEEE Trans. Antennas Propag.*, vol. 58, no. 2, pp. 340347, Feb. 2010.

[101] Y. Dong and T. Itoh, "Composite right/left-handed substrate integrated waveguide and half mode substrate integrated waveguide leaky-wave structures," *IEEE Trans. Antennas Propag.*, vol. 59, no. 3, pp. 767775, Mar. 2011.

[102] J. Liu, D. R. Jackson, and Y. Long, "Substrate integrated waveguide (SIW) leaky-wave antenna with transverse slots," *IEEE Trans. Antennas Propag.*, vol. 60, no. 1, pp. 2029, Jan. 2012.

[103] Y. J. Cheng, W. Hong, K.Wu, and Y. Fan, "Millimeter-wave substrate integrated waveguide long slot leaky-wave antennas and two-dimensional multibeam applications," *IEEE Trans. Antennas Propag.*, vol. 59, no. 1, pp. 4047, Jan. 2011.

[104] F. Xu and K. Wu, "Guided-wave and leakage characteristics of substrate integrated waveguide," *IEEE Trans. Microw. Theory Tech.*, vol. 53, no. 1, pp. 6673, Jan. 2005.

[105] K. A. Michalski and D. Zheng, "On the leaky modes of open microstrip lines," *Microw. Opt. Technol. Lett.*, vol. 2, no. 1, pp. 68, Jan. 1989.

[106] P. Baccarelli, C. Di Nallo, S. Paulotto, and D. R. Jackson, "A full wave numerical approach for modal analysis of 1D periodic microstrip structures," *IEEE Trans. Microw. Theory Tech.*, vol. 54, pp. 13501362, Apr. 2006.

[107] Theodoros N. Kaifas, "Uniform Asymptotic Solution for the Surface Magnetic Field Valid Both Within and Outside the Paraxial Region of a Perfect Electrically Conducting Circular Cylinder", *IEEE TRANSACTIONS ON ANTENNAS AND PROPAGATION*, VOL. 60, NO. 10, OCTOBER 2012

[108] R. F. Harrington, "Time-Harmonic Electromagnetic Fields". *New York: IEEE Press*, 2001.

[109] T. S. Bird, "Comparison of asymptotic solutions for the surface field excited by a magnetic dipole on a cylinder," *IEEE Trans. Antennas Propag.*, vol. AP-32, no. 11, pp. 12371244, Nov. 1984.

[110] Z. W. Chang, L. B. Felsen, and A. Hessel, "Surface ray methods for mutual coupling in conformal arrays on cylinder and conical surfaces," *Polytech. Inst.* New York, New York, NY, Final Rep., 1976.

[111] S. W. Lee and S. Safavi-Naini, "Asymptotic solution of surface field due to magnetic dipole on a cylinder," *Dept. Electr. Eng.*, Electromagn. Lab., Univ. Illinois at Urbana-Champaign, Urbana, IL, Rep. 76-11,1976.

[112] S. W. Lee and S. Safavi-Naini, "Approximate asymptotic solution of surface field due to a magnetic dipole on a cylinder," *IEEE Trans Antennas Propag.*, vol. AP-26, no. 4, pp. 593598, Jul. 1978.

[113] P. H. Pathak and N. Wang, "An analysis of the mutual coupling between antennas on a smooth convex surface," *ElectroSci. Lab., Dept. Electr. Eng.*, Ohio State Univ. , Columbus, OH, Rep. 784583-7, 1978.

[114] P. H. Pathak and N. Wang, "Ray analysis of mutual coupling between antennas on a convex surface," *IEEE Trans. Antennas Propag.*, vol. AP-29, no. 6, pp. 911922, Nov. 1981.

[115] J. Boersma and S.W. Lee, "Surface field due to a magnetic dipole on a cylinder: Asymptotic expansion of exact solution," *Dept. Electr. Eng.*, Electromagn. Lab., Univ. Illinois at Urbana-Champaign, Urbana, IL, Rep. 7817, 1978.

[116] T. S. Bird, "Accurate asymptotic solution for the surface field due to apertures in a conducting cylinder," *IEEE Trans. Antennas Propag.*, vol. AP-33, no. 10, pp. 11081117, Oct. 1985.

[117] Evert Slob and Kees Wapenaar, "Greens Function Extraction for Interfaces With Impedance Boundary Conditions", *IEEE TRANSACTIONS ON ANTENNAS AND PROPAGATION*, VOL. 60, NO. 1, JANUARY 2012

[118] E. Slob and K.Wapenaar, "Electromagnetic Greens functions retrieval by cross-correlation and cross-convolution in media with losses," *Geophys. Rev. Lett.*, vol. 34, no. 5, p. L05307, 2007.

[119] L. B. Liu and K. He, "Wave interferometry applied to borehole radar: Virtual multioffset reflection monitoring," *IEEE Trans. Geosci. Remote Sens.*, vol. 45, no. 8, pp. 25542559, Aug. 2007.

[120] E. Slob and K. Wapenaar, "GPR without a source: Cross-correlation and cross-convolution methods," *IEEE Trans. Geosci. Remote Sens.*, vol. 45, no. 8, pp. 25012510, Aug. 2007.

[121] E. Slob and K.Wapenaar, "Practical representations of electromagnetic interferometry for GPR applications: A tutorial," *Near Surface Geophys.*, vol. 6, no. 6, pp. 391402, Dec. 2008.

[122] E. Slob, "Interferometry by deconvolution of multi-component multioffset GPR data," *IEEE Trans. Geosci. Remote Sens.*, vol. 47, no. 3, pp. 828838, Mar. 2009.

[123] A. Kaufman and G. Keller, "Frequency and transient soundings," *Methods Geochem. Geophys.*. New York: Elsevier, 1983, vol. 16.

[124] Z. G. Qian, W. C. Chew, and R. Suaya, "Generalized impedance boundary condition for conductor modeling in surface integral equation," *IEEE Trans. Microw. Theory Tech.*, vol. 55, no. 11, pp. 2354-2364, Nov. 2007.

[125] O. zdemir, I. Akduman, A. Yapar, and L. Crocco, "Higher order inhomogeneous impedance boundary conditions for perfectly conducting objects," *IEEE Trans. Geosci. Remote Sens.*, vol. 45, no. 5, pt. 1, pp.1291-1297, May 2007.

[126] I. Hnninen and K. Nikoskinen, "Implementation of method of moments for numerical analysis of corrugated surfaces with impedance boundary condition," *IEEE Trans. Antennas Propagat.*, vol. 56, no. 1, pp. 278-281, Jan. 2008.

[127] M. F. Ctedra, C. Delgado, and I. G. Diego, "New physical optics approach for an efficient treatment of multiple bounces in curved bodies defined by an impedance boundary condition," *IEEE Trans. Antennas Propagat.*, vol. 56, no. 3, pp. 728736, Mar. 2008.

[128] J. Komijani and J. Rashed-Mohassel, "Symmetrical properties of dyadic Greens functions for mixed boundary conditions and integral representations of the electric fields for problems involving a PEMC," *IEEE Trans. Antennas Propagat.*, vol. 57, no. 10, pt. Part 2, pp. 31993204, Oct. 2009.

[129] S. Yuferev and L. Di Rienzo, "Surface impedance boundary conditions in terms of various formalisms," *IEEE Trans. Magn.*, vol. 46, no. 9, pp. 36173628, Sep. 2010.

[130] P. Yla-Oijala, S. P. Kiminki, and S. Jarvenpaa, "Solving IBC-CFIE with dual basis functions," *IEEE Trans. Antennas Propagat.*, vol. 58, no. 12, pp. 39974004, Dec. 2010.

[131] Y. Z. Umul and U. Yalcin, "The effect of impedance boundary conditions on the potential function of the boundary diffractionwave theory," *Opt. Commun.*, vol. 281, no. 1, pp. 2327, Jan. 2008.

[132] R. B. Clipp and B. N. Steele, "Impedance boundary conditions for the pulmonary vasculature including the effects of geometry, compliance, and respiration," *IEEE Trans. Biomed. Eng.*, vol. 56, no. 3, pp. 862870, Mar. 2009.

[133] D. Khaliullin and S. Tretyakov, "Generalized impedance-type boundary conditions for thin planar layers of various media (review)," *J. Commun. Technol. Electron.*, vol. 43, no. 1, pp. 1225, Jan 1998.

[134] V. Galdi and I. M. Pinto, "Derivation of higher-order impedance boundary conditions for stratified coatings composed of inhomogeneous-dielectric and homogeneous-bianisotropic layers," *Radio Sci.*, vol. 35, pp. 287303, 2000.

[135] J. Kong, "Theorems of bianisotropic media," *Proc. IEEE*, vol. 60, no.9, pp. 10361046, Sep. 1972.

[136] W. W. Chow, J. Gea-Banacloche, L. M. Pedrotti, V. E. Sanders, W. Schleich, and M. O. Scully, "The ring laser gyro," *Rev. Modern Phys.*, vol. 57, no. 1, pp. 61104, Jan. 1985.

[137] E. Slob and K. Wapenaar, "Retrieving the Greens function from cross correlation in a bianisotropic medium," *Progr. Electromagn. Res.-PIER*, vol. 93, pp. 255274, 2009.

[138] Ben Lai, Xun-Wang Zhao, Zi-Jian Su, and Chang-Hong Liang, "Higher Order MoM Analysis of the Rectangular Waveguide Edge Slot Arrays", *IEEE TRANSACTIONS ON ANTENNAS AND PROPAGATION*, VOL. 59, NO. 11, NOVEMBER 2011.

[139] I. Lindell and A. Sihvola, "Generalized soft-and-hard surface," *IEEE Trans. Antennas Propagat.*, vol. 50, no. 7, pp. 926929, Jul. 2002.

[140] I. Lindell and A. Sihvola, "Realization of the PEMC boundary," *IEEE Trans. Antennas Propagat.*, vol. 53, no. 9, pp. 30123018, Sep. 2005.

[141] I. Lindell, A. Sihvola, and K. Suchy, "Six-vector formalism in electromagnetics of bi-anisotropic media," *J. Electromagn. Waves Appl.*, vol. 9, no. 78, pp. 887903, 1995.

[142] K.Wapenaar, E. Slob, and J. Fokkema, "Reciprocity and power balance for piecewise continuous media with imperfect interfaces," *J. Geophys.* Res. B, vol. 109, no. 10, p. B10301, 2004.

[143] D. Hoppe and Y. Rahmat-Samii, "Impedance Boundary Conditions in Electromagnetics". *Bristol*, PA: Taylor and Francis, 1995.

[144] V. Rumsey, "Reaction concept in electromagnetic theory," *Phys. Rev.*, vol. 94, pp. 14831491, 1954.

[145] K. Wapenaar, E. Slob, and R. Snieder, "Unified Greens function retrieval by cross correlation," *Phys. Rev. Lett.*, vol. 97, no. 23, pp. 234301-1234301-4, 2006.

[146] K.Wapenaar, "General wave field representations for seismic modeling and inversion," *Geophysics*, vol. 72, no. 5, pp. SM5SM17, 2007.

[147] E. Slob, D. Draganov, and K. Wapenaar, "Interferometric electromagnetic Greens functions representations using propagation invariants," *Geophys. J. Int.*, vol. 169, no. 1, pp. 6080, 2007.

[148] I. V. Lindell and A. H. Sihvola, "Losses in the PEMC boundary," *IEEE Trans. Antennas Propagat.*, vol. 54, no. 9, pp. 25532558, Sep. 2006.

[149] Ben Lai, Xun-Wang Zhao, Zi-Jian Su, and Chang-Hong Liang, "Higher-Order MoM Analysis of the Rectangular Waveguide Edge Slot Arrays", *IEEE TRANSACTIONS ON ANTENNAS AND PROPAGATION*, VOL. 59, NO. 11, NOVEMBER 2011

[150] A. F. Stevenson, "Theory of slots in rectangular waveguides," *J. Appl. Phys.*, vol. 19, pp. 2438, Jan. 1948.

[151] B. N. Das, J. Ramakrishna, and B. K. Sarap, "Resonant conductance of inclined slots in the narrow wall of a rectangular waveguide," *IEEE Trans. Antennas Propag.*, vol. 32, pp. 759761, Jul. 1984.

[152] P. Hsu and S. H. Chen, "Admittance and resonance length of inclined slots in the narrow wall of rectangular waveguide," *IEEE Trans. Antennas Propag.*, vol. 37, pp. 4549, Jan. 1989.

[153] K. J. Xia, "Study of the inclined slots in the narrow wall of a rectangular waveguide," (in Chinese) *Ph.D. dissertation*, Dept. of Electronic Engineering, Tsinghua University, Beijing, China, 1990.

[154] C. G. Jan, P. Hsu, and R.-B. Wu, "Moment method analysis of sidewall inclined slot in rectangular waveguides," *IEEE Trans. Antennas Propag.*, vol. 39, pp. 6873, Jan. 1991.

[155] C. G. Jan, R. B.Wu, and P. Hsu, "Variational analysis of inclined slots in the narrow wall of a rectangular waveguide," *IEEE Trans. Antennas Propag.*, vol. 42, no. 10, pp. 14551458, Oct. 1994.

[156] C. G. Jan, R.-B.Wu, P. Hsu, and D. C. Chang, "Analysis of edge slots in rectangular waveguide with finite waveguide wall thickness," *IEEE Trans. Antennas Propag.*, vol. 44, no. 8, pp. 11201126, Aug. 1996.

[157] V. V. S. Prakash, S. Christopher, and N. Balakrishnan, "Sidewall inclined slot in a rectangular waveguide: Theory and experiment," *IEE Proc. H*, vol. 145, no. 3, pp. 233238, Jun. 1998.

[158] V. V. S. Prakash, S. Christopher, and N. Balakrishnan, "Method-of moments analysis of the narrow-wall slot array in a rectangular waveguide," *IEE Proc. H*, vol. 147, no. 3, pp. 242246, Jun. 2000.

[159] J. C. Young, J. Hirokawa, and M. Ando, "Analysis of a rectangular waveguide, edge slot array with finite wall thickness," *IEEE Trans. Antennas Propag.*, vol. 55, no. 3, pp. 812819, Mar. 2007.

[160] V. Catina and F. Arndt, "Rigorous surface integral method-of-moment analysis of rectangular waveguide edge-slot arrays," *in Proc. IEEE Antennas and Propagation Society Int. Symp.*, Jul. 2006, pp. 31453148.

[161] X. W. Zhao, Y. Zhang, T. K. Sarkar, and C. H. Liang, "Analysis of a traveling-wave waveguide array with narrow-wall slots using higher order basis functions in method of moments," *IEEE Antennas Wireless Propag. Lett.*, vol. 8, pp. 13901393, 2009.

[162] R. F. Harrington, "Field Computation by Moment Methods". *NewYork: Wiley*-IEEE, 1993.

[163] E. Jrgensen, J. L. Volakis, P. Meincke, and O. Breinbjerg, "Higher order hierarchical Legendre basis functions for electromagnetic modeling," *IEEE Trans. Antennas Propag.*, vol. 52, no. 11, pp. 29852995, Nov. 2004.

[164] Fu-Gang Hu, Member, IEEE, and Chao-Fu Wang, "Modeling of Waveguide Structures Using DG-FETD Method With Higher Order Tetrahedral Elements", *IEEE TRANSACTIONS ON MICROWAVE THEORY AND TECHNIQUES*, VOL. 60, NO. 7, JULY 2012

[165] M. Hano, "Finite-element analysis of dielectric-loaded waveguides," *IEEE Trans. Microw. Theory Tech.*, vol. 32, no. 10, pp. 12751279, Oct. 1984.

[166] J. F. Lee, D. K. Sun, and Z. J. Cendes, "Full-wave analysis of dielectric waveguides using tangential vector finite elements," *IEEE Trans. Microw. Theory Tech.*, vol. 39, no. 8, pp. 12621271, Aug. 1991.

[167] K. Ise, K. Inoue, and M. Koshiba, "Three-dimensional finite-element method with edge elements for electromagnetic waveguide discontinuities," *IEEE Trans. Microw. Theory Tech.*, vol. 39, no. 10, pp. 12891295, Oct. 1991.

[168] J. M. Jin, "The Finite Element Method in Electromagnetics", 2nd ed. *New York: Wiley*, 2002.

[169] L. T. Pillage and R. A. Rohrer, "Asymptotic waveform evaluation for timing analysis," *IEEE Trans. Comput.-Aided Design Integr. Circuits Syst.*, vol. 9, no. 4, pp. 352366, Apr. 1990.

[170] R. D. Graglia, D. R. Wilton, and A. F. Peterson, "Higher order interpolatory vector bases for computational electromagnetics," *IEEE Trans. Antennas Propag.*, vol. 45, no. 3, pp. 329342, Mar. 1997.

[171] J. P.Webb, "Hierarchal vector basis functions of arbitrary order for triangular and tetrahedral finite elements," *IEEE Trans. Antennas Propag*, vol. 47, no. 8, pp. 12441253, Aug. 1999.

[172] J. Liu, J.M. Jin, E. K. N. Yung, and R. S. Chen, "A fast three-dimensional higher-order finite element analysis of microwave waveguide devices," *Microw. Opt. Technol. Lett.*, vol. 32, pp. 344352, Mar. 2002.

[173] S. D. Gedney and U. Navsariwala, "An unconditionally stable finite-element time-domain solution of the vector wave equations," *IEEE Microw. Guided Wave. Lett.*, vol. 5, no. 5, pp. 332334, May 1994.

[174] J. F. Lee, R. Lee, and A. C. Cangellaris, "Time-domain finite element methods," *IEEE Trans. Antennas Propag.*, vol. 45, no. 3, pp. 430442, Mar. 1997

[175] D. Jiao, A. Ergin, B. Shanker, E. Michielssen, and J. M. Jin, "A fast time-domain higher-order finite element-boundary integral method for three-dimensional electromagnetic scattering analysis," *IEEE Trans. Antennas Propag.*, vol. 50, no. 9, pp. 11921202, Sep. 2002.

[176] M. Feliziani and F. Maradei, "Hybrid finite element solution of time dependent Maxwells curl equations," *IEEE Trans. Magn.*, vol. 31, no.3, pp. 13301335, May 1995.

[177] R. N. Rieben, G. H. Rodrigue, and D. A. White, "A high-order mixed vector finite element method for solving the time dependent Maxwell equations on unstructured grids," *J. Comput. Phys.*, vol. 204, pp. 490519, 2005.

[178] H.-p. Tsai, Y. Wang, and T. Itoh, "An unconditionally stable extended (USE) finite-element time-domain solution of active nonlinear microwave circuits using perfectly matched layers," *IEEE Trans. Microw. Theory Tech.*, vol. 50, no. 10, pp. 22262232, Oct. 2002.

[179] T. V. Yioultsis, N. V. Kantartzis, C. S. Antonopoulos, and T. D. Tsiboukis, "A fully explicit whitney-element time-domain scheme with higher order vector finite elements for three-dimensional high-frequency problems," *IEEE Trans. Magn.*, vol. 34, no. 5, pp. 32883291, Sep. 1998.

[180] B. He and F. L. Teixeira, "A sparse and explicit FETD via approximate inverse Hodge (mass) matrix," *IEEE Microw. Wireless Compon. Lett.*, vol. 16, no. 6, pp. 348350, Jun. 2006.

[181] B. Cockburn, G. E. Karniadakis, and C. W. Shu, "Discontinuous Galerkin Methods: Theory, Computation and Applications". *Berlin, Germany: Springer-Verlag*, 2000.

[182] J. S. Hesthaven and T. Warburton, "Nodal high-order methods on unstructured grids- I: Time-domain solution of Maxwells equations," *J. Comput. Phys.*, vol. 181, pp. 186211, 2002.

[183] T. Lu, P.W. Zhang, and W. Cai, "Discontinuous Galerkin methods for dispersive and lossy Maxwells equations and PML boundary conditions," *J. Comput. Phys.*, vol. 200, pp. 549580, 2004.

[184] T. Xiao and Q. H. Liu, "Three-dimensional unstructured-grid discontinuous Galerkin methods for Maxwells equations with well-posed perfectly matched layer," *Microw. Opt. Technol. Lett*, vol. 46, pp. 459463, Sep. 2005.

[185] L. Fezoui, S. Lanteri, S. Lohrengel, and S. Piperno, "Convergence and stability of a discontinuous Galerkin time-domain method for the 3-D heterogeneous Maxwell equations on unstructured meshes," *ESAIM: M2AN*, vol. 39, no. 6, pp. 11491176, Nov. 2005.

[186] B. Donderici and F. L. Teixeira, "Mixed finite-element time-domain method for transient Maxwell equations in doubly dispersive media," *IEEE Trans. Microw. Theory Tech.*, vol. 56, pp. 113120, Jan. 2008.

[187] R. Rieben,D.White, and G. Rodrigue, "High-order symplectic integration methods for finite element solutions to time dependent Maxwell equations," *IEEE Trans. Antennas Propag.*, vol. 52, pp. 21902195, Aug. 2004.

[188] S. D. Gedney, C. Luo, J. A. Roden, R. D. Crawford, B. Guernsey, J. A. Miller, T. Kramer, and E. W. Lucas, "The discontinuous Galerkin finite-element time-domain method solution of Maxwells equations," *ACES J.*, vol. 24, pp. 129141, Apr. 2009.

[189] S. Dosopoulos and J. F. Lee, "Interior penalty discontinuous Galerkin finite element method for the time-dependent first order Maxwells equations," *IEEE Trans. Antennas Propag.*, vol. 58, no. 12, pp. 4085-4090, Dec. 2010.

[190] Z. Lou and J. M. Jin, "A new explicit time-domain finite-element method based on element-level decomposition," *IEEE Trans. Antennas Propag.*, vol. 54, no. 10, pp. 29902999, Oct. 2006.

[191] J. M. Jin, K. C. Donepudi, J. Liu, G. Kang, J. Song, and W. C. Chew, "High-order methods in computational electromagentics," *Fast and Efficient Algorithms in Computational Electromagnetics*, W. C. Chew,Ed. et al. Norwood, MA: Artech House, 2001

[192] F. G. Hu, C. F. Wang, and Y. B. Gan, "Efficient calculation of interior scattering from large three-dimensional PEC cavities," *IEEE Trans. Antennas Propag.*, vol. 55, no. 1, pp. 167177, Jan. 2007.

[193] E. Montseny, S. Pernet, X. Ferrires, and G. Cohen, "Dissipative terms and local time-stepping improvements in a spatial high order discontinuous Galerkin scheme for the time-domainMaxwells equations," *J. Comput. Phys.*, vol. 227, pp. 67956820, 2008.

[194] J. P. Berenger, "A perfectly matched layer for the absorption of electromagnetic waves," *J. Comput. Phys.*, vol. 114, pp. 195200, 1994.

[195] W. C. Chew and W. H. Weedon, "A 3-D perfectly matched medium from modified Maxwells equations with stretched coordinates," *Microw. Opt. Technol. Lett.*, vol. 7, pp. 599604, 1994.

[196] S. D. Gedney, "Perfectly matched layer absorbing boundary conditions," *Computational Electrodynamics: The Finite-Difference Time-Domain Method*, A. Taflove and S. B. Hagness, Eds., 3rd ed. Boston, MA: Artech House, 2005.

[197] T. H. Loh and C. Mias, "Implementation of an exact modal absorbing boundary termination condition for teh application of the finite-element time-domain technique to discontinuity problems in closed homogeneous waveguides," *IEEE Trans. Microw. Theory Tech.*, vol. 52, no. 3, pp. 882888, Mar. 2004.

[198] Z. Lou and J. M. Jin, "An accurate waveguide port boundary condition for the time-domain finite-element method," *IEEE Trans. Microw. Theory Tech.*, vol. 53, no. 9, pp. 30143023, Sep. 2005.

[199] A. Zhao and V. Risnen, "Application of a simple and efficient source excitation technique to the FDTD analysis of waveguide and microstrip circuits," *IEEE Trans. Microw. Theory Tech.*, vol. 44, no. 9, pp. 15351539, Sep. 1996.

[200] S. P. Yeo, L. Qiao, and M. Cheng, "Symmetrical -port waveguide junction loaded with dielectric sleeve and metallic post," *IEEE Trans. Microw. Theory Tech.*, vol. 43, no. 6, pp. 12981302, Jun. 1995.

[201] J. Maloney, G. Smith, and W. Scott, "Accurate computation of the radiation from simple antennas using the finite difference time-domain method," *IEEE Trans. Antennas Propag.*, vol. 38, no. 7, pp.1059-1068, Jul. 1990.

[202] Iigo Liberal, Student Member, IEEE, Iigo Ederra, Cristina Gmez-Polo, Alberto Labrador, Jose Ignacio Prez-Landazbal, and Ramn Gonzalo, "A Comprehensive Analysis of the Absorption Spectrum of Conducting Ferromagnetic Wires", *IEEE TRANSACTIONS ON MICROWAVE THEORY AND TECHNIQUES*, VOL. 60, NO. 7, JULY 2012

[203] S. A. Baranov, "Use of a microconductor with natural ferromagnetic resonance for radio-absorbing materials," *Tech. Phys. Lett.*, vol. 24, no.7, pp. 549550, Jul. 1998.

[204] P. Marin, D. Cortina, and A. Hernando, "Electromagnetic wave absorbing material based on magnetic microwires," *IEEE Trans. Magn.*, vol. 44, no. 11, pp. 39343937, Nov. 2008.

[205] Z. Zhang, C.Wang, Y. Zhang, and J. Xie, "Microwave absorbing properties of composites filled with glass-coated Fe Co Si B amorphous microwire," *Mater. Sci. Eng. B*, vol. 175, no. 3, pp. 233237, Dec. 2010.

[206] D. P. Makhnovskiy and L. V. Panina, "Experimental demonstration of tunable scattering spectra at microwave frequencies in composite media

containing CoFeCrSiB glass-coated amorphous ferromagnetic wires and comparison with theory," *Phys. Rev. B, Condens. Matter*, vol. 74, no. 6, pp. 111, Aug. 2006.

[207] F. X. Qin, N. Pankratov, H. X. Peng, M. H. Phan, L. V. Panina, M. Ipatov, V. Zhukova, A. Zhukov, and J. Gonzalez, "Novel magnetic microwires- embedded composites for structural health monitoring applications," *J. Appl. Phys.*, vol. 107, no. 9, 2010, Art. ID 09A314.

[208] S. Starostenko and K. N. Rozanov, "Microwave screen with magnetically controlled attenuation," *Progr. Electromagn. Res.*, vol. 99, pp. 405426, 2009.

[209] I. Liberal, I. S. Nefedov, I. Ederra, R. Gonzalo, and S. A. Tretyakov, "Electromagnetic response and homogenization of grids of ferromagneticmicrowires," *J. Appl. Phys.*, vol. 110, no. 6, 2011, Art. ID 064909.

[210] I. Liberal, I. S. Nefedov, I. Ederra, R. Gonzalo, and S. A. Tretyakov, "On the effective permittivity of arrays of ferromagnetic wires," *J. Appl. Phys.*, vol. 110, no. 10, 2011, Art. ID 104902.

[211] D. P. Makhnovskiy and L. V. Panina, "Field dependent permittivity of composite materials containing ferromagnetic wires," *J. Appl. Phys.*, vol. 93, no. 7, 2003, Art. ID 4120.

[212] L. V. Panina, M. Ipatov, V. Zhukova, A. Zhukov, and J. Gonzalez, "Magnetic field effects in artificial dielectrics with arrays of magnetic wires at microwaves," *J. Appl. Phys.*, vol. 109, no. 5, 2011, Art. ID 053901.

[213] O. Reynet, A. Adenot-Engelvin, S. Deprot, O. Acher, and M. Latrach, "Effect of the magnetic properties of the inclusions on the high-frequency dielectric response of diluted composites," *Phys. Rev. B, Condens. Matter*, vol. 66, no. 9, pp. 19, Sep. 2002.

[214] V. Boucher and D. Mnard, "Effective magnetic properties of arrays of interacting ferromagnetic wires exhibiting gyromagnetic anisotropy and retardation effects," *Phys. Rev. B, Condens. Matter*, vol. 81, no.17, pp. 121, May 2010.

[215] S. E. Lofland, H. Garca-Miquel, M. Vzquez, and S. Bhagat, "Microwave magnetoabsorption in glass-coated amorphous microwires with radii close to skin depth," *J. Appl. Phys.*, vol. 92, no. 4, 2002, Art. ID 2058.

[216] L. Kraus, G. Infante, Z. Frait, and M. Vzquez, "Ferromagnetic resonance in microwires and nanowires," *Phys. Rev. B, Condens. Matter*, vol. 83, no. 17, pp. 44384449, May 2011.

[217] F. Yildiz, B. Z. Rameev, S. I. Tarapov, L. R. Tagirov, and B. Aktas, "High-frequency magnetoresonance absorption in amorphous magnetic microwires," *J. Magn. Magn. Mater.*, vol. 247, no. 2, pp. 222229, Jun. 2002.

[218] G. Goglio, S. Pignard, A. Radulescu, L. Piraux, I. Huynen, D. Vanhoenacker, and A. V. Vorst, "Microwave properties of metallic nanowires," *Appl. Phys. Lett.*, vol. 75, no. 12, pp. 17691772, 1999.

[219] H. Garca-Miquel, M. Esbri, J. Andres, J. Garcia, J. Garcia-Beneytez, and M. Vzquez, "Power absorption and ferromagnetic resonance in Co-rich metallic glasses," *IEEE Trans. Magn.*, vol. 37, no. 1, pp.561564, 2001.

[220] N.-E. Belhadj-Tahar, A. Fourrier-Lamer, and H. de Chanterac, "Broadband simultaneous measurement of complex permittivity and permeability using a coaxial discontinuity," *IEEE Trans. Microw. Theory Tech.*, vol. 38, no. 1, pp. 17, Jan. 1990.

[221] J. Garcia-Beneytez, F. Vinai, L. Brunetti, H. Garca-Miquel, and M. Vzquez, "Study of magneto impedance effect in the microwave frequency range for soft magnetic wires and microwires," *Sens. Actuators A, Phys.*, vol. 81, no. 13, pp. 7881, Apr. 2000.

[222] L. Kraus, "Theory of ferromagnetic resonances in thin wires," *Czech. J. Phys.*, vol. 32, no. 11, pp. 12641282, Nov. 1982.

[223] I. Liberal, I. Ederra, C. Gmez-Polo,A. Labrador, J. Prez-Landazabal, and R. Gonzalo, "Theoretical modeling and experimental verification of the scattering from a ferromagnetic microwire," *IEEE Trans. Microw. Theory Tech.*, vol. 59, no. 3, pp. 517526, Mar. 2011.

[224] Hao Wang, Member, IEEE, Da-Gang Fang, Fellow, IEEE, Bing Zhang, and Wen-Quan Che, Member, "Dielectric Loaded Substrate Integrated Waveguide (SIW) -Plane Horn Antennas", *IEEE TRANSACTIONS ON ANTENNAS AND PROPAGATION*, VOL. 58, NO. 3, MARCH 2010

[225] D. Deslandes and K. Wu, "Integrated transition of coplanar to rectangular waveguides," *IEEE MTT-S Int. Microwave Symp. Dig.*, Feb. 2001, pp. 619622.

[226] Y. Cassivi et al., "Dispersion characteristics of substrate integrated rectangular waveguide," *IEEE Microw. Wireless Compon. Lett.*, vol. 12, no. 9, pp. 333335, 2002.

[227] C.-H. Tseng and T.-H. Chu, "Measurement of frequency-dependent equivalent width of substrate integrated waveguide," *IEEE Trans. Microw. Theory Tech.*, vol. 54, no. 4, pp. 14311437, 2006.

[228] F. Xu and K. Wu, "Guided-wave and leakage characteristics of substrate integrated waveguide," *IEEE Trans. Microw. Theory Tech.*, vol. 53, no. 1, pp. 6673, 2005.

[229] D. Deslande and K. Wu, "Single-substrate integration technique ofplanar circuits and waveguide filters," *IEEE Trans. Microw. Theory Tech.*, vol. 51, no. 2, pp. 593596, 2003.

[230] A. Zeid and H. Baudrand, "Electromagnetic scattering by metallic holes and its applications in microwave circuit design," *IEEE Trans. Microw. Theory Tech.*, vol. 50, no. 4, pp. 11981206, 2002.

[231] L. Yan et al., "Simulation and experiment on SIW slot array antenna," *IEEE Microw.Wireless Compon. Lett.*, vol. 14, no. 9, pp. 446448, 2004.

[232] D. Deslandes and K.Wu, "Integrated microstrip and rectangular waveguide in planar form," *IEEE Microw. Wireless Compon. Lett.*, vol. 11, pp. 6870, 2001.

[233] F. Xu, K.Wu, and W. Hong, "Domain-decomposition FDTD algorithm combined with numerical TL calibration technique and its application in parameter extraction of substrate integrated," *IEEE Trans. Microw. Theory Tech.*, vol. 54, no. 1, pp. 329338, 2006.

[234] Z. L. Li and K. Wu, "An new approach to integrated horn antenna," *Proc. Int. Symp. on Antenna Technology and Applied Electromagnetics*, Jul. 2004, pp. 535538.

[235] R. E. Collin and F. J. Zucker, "Antenna Theory, Part 2". *New York:* McGraw-Hill, 1969.

[236] L. Xue and V. Fusco, "Patch fed planar dielectric slab extended hemielliptical lens antenna," *IEEE Trans. Antennas Propag.*, vol. 56, no. 3, pp. 661666, 2008

[237] Fernando L. Teixeira, "Time-Domain Finite-Difference and Finite-Element Methods for Maxwell Equations in Complex Media", *IEEE TRANSACTIONS ON ANTENNAS AND PROPAGATION*, VOL. 56, NO. 8, AUGUST 2008

[238] K. S. Kunz and R. J. Luebbers, "Finite Difference Time Domain Method for Electromagnetics." *Boca Raton, FL*: CRC Press, 1993.

[239] "A. Taflove, Computational Electrodynamics: The Finite-Difference Time-Domain Method". *Norwood, MA*: Artech House, 1995.

[240] "D. M. Sullivan, Electromagnetic Simulation using the FDTD Method". *New York*: IEEE Press, 2000.

[241] J. M. Jin, "The Finite Element Method in Electromagnetics". *New York*:Wiley, 1993.

[242] P. P. Silvester and G. Pelosi, "Finite Elements for Wave Electromagnetics: Methods and Techniques". *New York*: IEEE Press, 1994.

[243] P. P. Silvester and R. L. Ferrari, "Finite Elements for Electrical Engineers". *Cambridge, U.K.*: Cambridge Univ. Press, 1996.

[244] A. Bossavit, "Computational Electromagnetics: Variational Formulations, Complementarity, Edge Currents". *San Diego, CA*: Academic, 1998.

[245] J. L. Volakis, A. Chatterjee, and L. C. Kempel, "Finite Element Method for Electromagnetics: Antennas, Microwave Circuits, and Scattering Applications". *New York*: IEEE Press, 1998.

[246] "P. Monk, Finite Element Methods for Maxwells Equations". *Oxford, U.K.*: Oxford Univ. Press, 2003.

[247] B. Fornberg, "A Practical Guide to Pseudospectral Methods". *Cambridge, U.K.*: Cambridge Univ. Press, 1998.

[248] Q. H. Liu, "Large-scale simulations of electromagnetic and acoustic measurements using the pseudospectral time-domain (PSTD) algorithm," *IEEE Trans. Geosci. Remote Sens.*, vol. 37, no. 2, pp. 917926, 1999.